Analytical formulations for nitrogen oxides emissions estimation of a hydrogen fueled Synergetic Air-Breathing Rocket Engine (SABRE) in air-breathing mode

Acta Astronautica 228 (2025) 42–57

Contents lists available at ScienceDirect

Acta Astronautica

journal homepage: www.elsevier.com/locate/actaastro

Analytical formulations for nitrogen oxides emissions estimation of a hydrogen fueled Synergetic Air-Breathing Rocket Engine (SABRE) in air-breathing mode

Roberta Fusaro [a], Fabrizio Borgna [a,*], Nicole Viola [a], Guido Saccone [b]

[a] Politecnico di Torino, Corso Duca degli Abruzzi 24, 10129, Turin, Italy
[b] Italian Aerospace Research Centre, Via Maiorise, 81043, Capua, Italy

ARTICLE INFO

Keywords:
Reusable launchers
Air-breathing propulsive technologies
High-speed
Hydrogen combustion
Nitrogen oxides emission estimation
Synergetic air-breathing rocket engine
P3T3 method
Fuel flow method

ABSTRACT

The space sector is undergoing rapid expansion due to the transformations it is experiencing, evolving from government-funded traditional space initiatives to commercially driven NewSpace activities. The surge of government and private investments in the space domain has positioned it as one of the world's fastest-growing sectors, making it crucial to assess the impact of already operational launch assets and to adopt design-to-sustainability strategies for under-development and future launchers. To actively contribute to this transition, this paper proposes a methodology for deriving novel analytical formulations to estimate nitrogen oxide (NO_x) emissions of a hydrogen-fueled reusable access-to-space vehicle. Throughout the paper, the Skylon spaceplane and its Synergetic Air Breathing Rocket Engine are used as a case study. In particular, the SABRE engine presents a highly integrated dual propulsion architecture supporting both air-breathing and rocket modes. This study specifically focuses on the former, enabling the Single Stage To Orbit (SSTO) Skylon reaching the hypersonic speed regime before transitioning to rocket mode. This paper proposes novel analytical formulations to be integrated into the Fuel Flow (FF) and P3-T3 methods for estimating NO_x Emission Index ($EINO_x$), since the early design phase. These estimation techniques currently enable the calculation of the emission index of pollutants and GreenHouse Gases (GHGs) produced by any subsonic aero-engines powered by traditional fuels (i.e. kerosene) only. The methodology presented in this paper allows for upgrading the original mathematical formulations of the methods to ensure the applicability to high-speed flight and hydrogen fuel conditions. This involves the propulsive modelling of the engine and the chemical-kinetic modelling of the combustion process, representative of various on-ground and in-flight operating conditions, to generate updated and reliable propulsive and emissive databases for the engine. To this end, 0D chemical-kinetic air/hydrogen combustion numerical simulations are employed. The results of the performance analysis and emission modeling of the SABRE engine are reported and discussed. Regarding the calculated $EINO_x$ trend for the air-breathing phase of the engine operation, it reaches a peak of 45 $g_{NOx}/kg_{H2burnt}$ under hypersonic conditions. Through the analysis of correlations between the propulsive characteristics of the SABRE and its NO_x production, a series of parameters (such as Mach Number, Fuel to Air Ratio, Water to Fuel Ratio, and others) are selected to be integrated into the original formulations of the P3-T3 and FF methods via mathematical interpolation to adapt them to the case study. Finally, the $EINO_x$ trends resulting from the application of the new H2-P3T3 and H2-FF methods to the SABRE are graphically reported, along with the corresponding estimation errors relative to the reference trend from the engine emission database. Additionally, a discussion regarding the chemical-physical justifications for the mathematical contributions to the formulations for $EINO_x$ of the newly introduced parameters is provided.

* Corresponding author.
E-mail addresses: roberta.fusaro@polito.it (R. Fusaro), fabrizio.borgna@studenti.polito.it (F. Borgna), nicole.viola@polito.it (N. Viola), g.saccone@cira.it (G. Saccone).

https://doi.org/10.1016/j.actaastro.2024.11.061
Received 31 October 2024; Received in revised form 29 November 2024; Accepted 30 November 2024
Available online 2 December 2024

Nomenclature

δ	Pressure ratio between FL and SL standard conditions
θ	Temperature ratio between FL and SL standard conditions
p_3	Pressure at the inlet of the combustion chamber
T_3	Temperature at the inlet of the combustion chamber
Acronyms/Abbreviations	
BFFM2	Boeing Fuel Flow Method 2
CC	Combustion Chamber
CO	Carbon monoxide
CO_2	Carbon dioxide
COP	Conference of the Parties
EI	Emission Index
FAR	Fuel to Air Ratio
FFM	Fuel Flow Method
FL	Flight Level
FT	Flame Temperature
GHG	GreenHouse Gases
H	Air humidity factor
H_2	Hydrogen fuel
H_2O	Water Vapor
H2–FFM	Hydrogen and High-speed FFM formulations
H2–P3T3	Hydrogen and High-speed P3T3 formulations
HE ratio	Ratio between He mass flow at the He turbine inlet and total air mass flow at the air compressor inlet powered by the He turbine
HeT	Helium turbine
HT	Hydrogen turbine
HX	Heat Exchanger
ICAO	International Civil Aviation Organization
ISA	International Standard Atmosphere
LEO	Low Earth Orbits
LES	Large Eddy Simulations
LH_2	Liquid Hydrogen fuel
LO_x	Liquid Oxygen propellant
M	Mach number
NO_x	Nitrogen Oxides
P3-T3	P3-T3 method
PB	Preburner
PBratio	Ratio between PB air mass flow and total air mass flow
REL	Reaction Engines Limited
SABRE	Synergetic Air Breathing Rocket Engine SL Sea level
UNCC	UN Climate Change Conference
USD	United States Dollars
WFR	Water to Fuel Ratio at the inlet of the combustion chamber
Y	Mass Fraction

1. Introduction

As global temperatures reached record highs and extreme weather events increasingly impacted communities around the world, the 28th Conference of the Parties (COP28), held from November 30th to December 12th, 2023, in Dubai, United Arab Emirates, served as an international forum to highlight the necessity of collective action in addressing the climate crisis. Participating governmental and international institutions produced the first global assessment of progress toward achieving the climate objectives outlined in the Paris Agreement to limit global warming to 1.5 °C by 2050. During the COP28 UN Climate Change Conference (UNCC), it was established the necessity to reach the peak of global GreenHouse Gas (GHG) emissions by 2025, followed by a 43 % reduction by 2030 and a 60 % reduction by 2035 compared to 2019 levels [1]. In this scenario of attention towards emissions reduction, the aerospace sector has proven to be one of the hardest to abate. The space industry, expected to exceed a global revenue of 1 trillion USD by 2040 [2,3], stands out as one of the world's fastest-growing sectors. In recent years, the global rocket engine sector has experienced significant growth due to increasing commercial, governmental, and scientific interest in space exploration. This rapid expansion is due to the transformation that the space field is experiencing, evolving from government-funded traditional space initiatives to commercially driven NewSpace ventures [4]. This era has marked a historic shift in the space domain, transforming it from a government-dominated sector to a dynamic, competitive one that attracts private market allocations [5]. This surge has resulted in a notable increase in annual space launches, causing concerns regarding both the accumulation of space debris in orbit and the cascading effect known as the Kessler syndrome, as well as the chemical emissions from space access vehicles [6,7]. Alongside the concerns regarding space debris, the rapid expansion of space-related activities has led to increased emissions in the upper atmosphere, where the residence times of emitted species vary, and the environmental impact of emissions, particularly nitrogen oxides (NO_x), proves to be critical [6]. Assessing the Aerospace Sector Emission Index (ASEI) has thus become increasingly critical to evaluate the magnitude of the potential impact of anthropogenic climate forcing and develop targeted strategies to curb emissions. In this regard, previous studies have shown that focusing solely on the impact of CO_2 emissions on stratospheric ozone depletion, while neglecting the broader range of pollutants and their interactions in the upper atmosphere, significantly underestimates the contribution of rockets to climate change [8]. In this context, emissions of water vapor (H_2O) and nitrogen oxide (NO_x) from rocket engines can contribute to the formation of polar mesospheric clouds and other climate-altering phenomena, which are still not fully understood [9]. The issue of high-altitude emissions raises concerns not only in the domain of space access but also within the aviation industry, especially regarding high-speed flights and future reusable access-to-space vehicles. For these advanced applications, Hydrogen (H_2) stands as a promising energy vector, given its high efficiency and zero-carbon combustion characteristics. The primary advantage of utilizing liquid hydrogen (LH_2) as a fuel lies in its exceptionally high gravimetric energy density, enabling the storage of significantly more energy compared to conventional fuels. However, when considering its volumetric energy density, other alternatives offer notably greater advantages. The production, handling, and particularly the storage of cryogenic hydrogen remain challenging due to the extreme pressure and temperature conditions required for its liquefaction and maintenance. Moreover, the high costs associated with liquefaction processes, cryogenic infrastructure, and material compatibility further complicate its widespread adoption [10]. Compared to other fuels, hydrogen exhibits a significantly higher laminar flame speed, which improves flame propagation and overall combustion efficiency. Consequently, hydrogen is often utilized as a combustion promoter to address the slower flame speeds of alternative fuels, optimizing performance even in fuel blends [11,12]. Indeed, H_2 offers the highest heat release and the shortest kinetic time among available fuels, with wide flammability limits (4–75 % in air), making it efficient and reliable in supersonic combustion engines [13,14]. Additionally, H_2 has optimal mixing characteristics, excellent cooling properties and it can be considered an ideal gas over a wide temperature range and even at high pressures, simplifying the modelling of its thermodynamic behaviour [15–18]. Regarding LH2-Air combustion, it produces only water and NO_x emissions, eliminating CO_2, CO, unburned hydrocarbons, and soot, making it environmentally advantageous. However, when non-CO_2 emissions resulting from hydrogen combustion occur in the stratosphere, as in the case of supersonic and hypersonic aircraft, they exhibit longer atmospheric lifetimes compared to emissions from subsonic aircraft, which predominantly operate within the troposphere. The consequences of these emissions, particularly those of NO_x, can be critical for the ozone layer, which acts as a shield for the Earth and influences global warming [19,20]. Indeed, NO_x emissions during high-speed flights at high altitudes can both increase and decrease ozone levels, depending on flight conditions, thus complicating the environmental implications [21–23]. Ongoing research activities on reusable access-to-space systems highlights a significant gap in established methodologies for accurately estimating emissions during the design phases. While adopting hydrogen as an alternative fuel is a key strategy to reduce environmental impact, assessing and addressing this impact comprehensively remains challenging.

The present paper discloses novel conceptual design formulations to predict pollutant and GHG emissions for hydrogen-fueled reusable

access-to-space vehicle during atmospheric flight, with a specific focus on nitrogen oxide emissions. Indeed, NO_x emissions are particularly important in hydrogen combustion, especially when occurring above the troposphere. However, the in-depth literature review reported in Section 2 reveals the following gaps:

(i) no analytical formulations are currently available to estimate emissions from hydrogen combustion;
(ii) no analytical formulations are currently available for combined-cycle engine for reusable space transportation
(iii) the applicability of available estimation methods has not been verified beyond the subsonic speed regime

Therefore, the goals of this paper are:

(i) to identify already available methods to be used as reference;
(ii) to reveal the limitations of already available methods for NOx estimation when applied to hydrogen fueled combined-cycle engines in high-speed regimes. Indeed, when they are applied to non-conventional engines—such as non-subsonic engines or those not fueled by kerosene—the resulting emission estimates exhibit significant divergence, yielding unrealistic trends unsupported by physical or chemical justification.;
(iii) to develop novel analytical formulations for a specific hydrogen fueled combined-cycle engine, namely the Synergetic Air Breathing Rocket Engine (SABRE) installed on the Skylon Single Stage To Orbit (SSTO).

In details, two NO_x emission index estimation methods (P3-T3 and FF methods), developed within the context of general aviation, have been selected to expand their applicability to the considered case study. In addition, this paper specifically examines the air-breathing phase of the engine, enabling the SSTO Skylon to reach hypersonic speeds before transitioning to rocket mode. To achieve these ambitious goals, the authors integrate simplified yet precise propulsive system models with 0D chemical-kinetic combustion models. These models are designed to be useful during the conceptual design phase by requiring only a minimal set of input data, consistent with the information typically available at this stage, and minimal computational resources, ensuring compatibility with rapid design iterations.

The paper begins with a comprehensive review of nitrogen oxide (NO_x) emission prediction techniques for traditional subsonic aeroengines and fuels, presented in Section 2, to evaluate their potential extension for high-speed air-breathing engines using hydrogen. Among all available methods, the analytical formulations proposed by the Fuel Flow and P3-T3 methods for estimating NO_x Emission Index ($EINO_x$) were selected for modification and adaptation to the characteristics of the case study, considering their applicability during the early design phases. These methods provide mathematical formulations for evaluating $EINO_x$ in Flight Level conditions (FL) based on $EINO_x$ data recorded at Sea Level conditions (SL), appropriately corrected using easily obtainable or estimable chemical-propulsive parameters during conceptual design, such as combustion chamber inlet pressures and temperatures (p_3, T_3), Fuel to Air Ratio (FAR), and fuel flow (w_f). Section 3 offers insights into the case study: the SABRE technology is described, and the propulsion and emissions models and databases available to the authors are discussed. From this state-of-the-art analysis, requirements for upgrading existing propulsion and emissions models were identified. Section 4 provides an in-depth description of the methodology developed to derive new formulations of the Fuel Flow and P3-T3 methods for high-speed aircraft using hydrogen (H2-FF, H2-P3T3). This strategy involves updating the propulsion model of the engine, recalculating the propulsive and emissive databases, and analysing the correlations between the chemical-propulsive parameters of the engine and its NO_x production. Once the two databases are updated, the adaptation of the methods is conducted by introducing additional parameters compared to the original formulations, selected based on a correlation-based approach. This strategy involved the study of correlations between the chemical-propulsive characteristics of the SABRE and the NO_x formation during the combustion process. This correlation analysis led to the selection of a set of key parameters that determine the flame temperature profile achieved during combustion, which was found to be the most influential factor in NO_x production within the combustion chamber. The parameters chosen for integration into the new formulations directly affect the flame temperature and were selected to represent the unique configuration of the SABRE combined cycle. These parameters include the Mach number, Fuel-to-Air ratio (FAR), airflow rate into the PreBurner (PBratio), water flow rate into the main Combustion Chamber, i.e., Water to Fuel Ratio (WFR), and helium flow rate utilized for regeneratively managing the engine thermal load (HEratio). These parameters, expressed as FL/SL ratios, feature in the new mathematical relationships that calculate the $EINO_{xFL}$ as a correction of the $EINO_{xSL}$. Each proposed new formulation entails a different combination of these parameters, yielding different curve-fitting optimization coefficients and consequently resulting in varying errors for the modified formulations. Thus, the progressive addition of parameters to the original formulations of the methods leads to a series of new formulations characterized by different levels of estimation accuracy. This allows for the selection of the most appropriate formulation to estimate the $EINO_x$ of the SABRE depending on the available data, including non-proprietary data, or based on the desired level of accuracy to be achieved. Finally, the updated mathematical formulations of the H2-FF and H2-P3T3 are applied to the case study as presented in Section 5. Additionally, the absolute and relative errors of the newly formulated H2-P3T3 and H2-FF models, calculated with respect to a subset of EINO data under flight-level conditions from the updated emissive database, are reported. This enables a comprehensive assessment of the estimation accuracy achieved by the two methods.

2. State of the art in NO_x emissions modelling for aeronautical applications

Numerous methodologies are available for estimating emissions of pollutants and greenhouse gases from the aviation sector, each requiring different input data and yielding varying levels of accuracy. According to Ref. [24], NO_x emission estimation methods can be categorized into five groups: (i) correlation-based models, (ii) P3-T3 methods, (iii) Fuel-Flow methods, (iv) simplified physics-based models, and (v) high-fidelity simulations. Following thorough investigations, the authors selected the P3-T3 method and the Fuel-Flow (FF) method, specifically its Boeing Fuel Flow Method 2 (BFFM2) variant, as a foundational framework for developing innovative predictive analytical formulations. Behind the selection of the P3-T3 and BFFM2 methods, the applicability of each method category in the conceptual design phase of high-speed aircraft propelled by liquid hydrogen is analysed. Correlation-based models assess the $EINO_x$ of the engine using empirical or semi-empirical relationships derived from correlations between NO_x emissions and primary or secondary propulsion-emission variables [25]. This data is integrated into mathematical formulations to estimate the NO_x Emission Index, utilizing a combination of parameters. However, achieving an acceptable accuracy in estimations with these methods necessitates using a considerable number of variables. Indeed, each variable is subject to detection or estimation errors, which accumulate when combined into a single formulation for the calculation of $EINO_x$. On the other hand, simplified physics-based models and high-fidelity simulations are excluded from this discussion due to their limitations and incompatibility with the conceptual design phase. These methods represent medium-to-high reliability tools for emissions prediction. Simplified physics-based models broadly describe the combustion process from a physical perspective by dividing the combustion chamber into distinct regions, each characterized by specific chemical concentrations and assumptions. This segmentation allows the chamber to be

modeled as a network of ideal reactors, leading to reduced computational costs by simplifying NO_x formation kinetics. While these models balance computational efficiency and predictive accuracy, they fail to capture the intricate kinetic pathways of pollutant formation, particularly limiting their application to hydrogen-powered aeronautical systems [26]. Conversely, high-fidelity simulations represent the most accurate approach for predicting emissions, requiring a detailed understanding of combustor geometry and NO_x formation kinetics. Common high-fidelity methods include Reynolds-Averaged Navier-Stokes (RANS) solutions, which require known combustor boundary conditions, Direct Numerical Simulations (DNS), which are computationally efficient but impractical for complex configurations, and Large-Eddy Simulations (LES), which incorporate small-scale turbulence modeling. The reliance of these simulation techniques on extensive specialized knowledge of the combustor, combined with their significant computational resource demands, presents substantial challenges during the conceptual design phase. For this reason, the methods selected for this study are P3-T3 and BFFM2, which represent two specializations of the correlation-based models characterized by a limited number of variables involved and acceptable accuracy. These methods calculate $EINO_x$ at flight level (FL) based on sea level (SL) measurements, corrected for altitude conditions. The P3-T3 method requires temperature and pressure profiles at the combustion chamber inlet, while FF methods use ambient conditions and fuel flow profiles. Furthermore, these methods feature unified coefficient formulations designed to apply to all types of subsonic aircraft engines powered by traditional fuels. Notably, the Fuel Flow (FF) methods are derived from the P3-T3 method, addressing the need for a methodology applicable even in the absence of proprietary engine data. There are two primary FF methods: the Boeing Fuel Flow Method 2 (BFFM2) developed by Boeing and the DLR Fuel Flow method developed by the German Aerospace Centre. These two formulations differ only in their exponential correction factors. Therefore, this paper will focus solely on the BFFM2, as it is more commonly referenced in the literature.

2.1. P3-T3 method

The P3-T3 method stands as the most used approach for estimating NO_x emission indices. This method directly stems from Correlation-Based Models, focusing on a limited range of parameters of interest, which include temperature and pressure at the inlet of the combustor (P_3, T_3), and the Fuel-to-Air Ratio (FAR). These variables are included in the compact mathematical formulation provided below.

$$EINO_{xFL} = EINO_{xSL}\left(\frac{p_{3FL}}{p_{3sL}}\right)^{n}\left(\frac{FAR_{FL}}{FAR_{sL}}\right)^{m}\exp(H) \quad (1)$$

$$H = 19^{*}(h_{SL} - h_{FL}) \quad (2)$$

where H represents the humidity factor, introduced to consider humidity impact on NO_x formation in the combustion chamber. As humidity rises, combustion temperature decreases, reducing NO_x production. The H factor is calculated based on the relative increase in specific humidity h due to altitude gain. Despite not being explicitly included, the combustor inlet temperature T_3 implicitly influences the application of the method and serves as a key parameter in the procedure documented in the literature [24]. The generalized formulation typically employs exponent coefficients (n = 0.4 and m = 0), but optimized coefficients can be used for specific cases to enhance accuracy. Despite the accuracy in estimating Emission Indices that this method offers, it requires access to proprietary engine data. If this data is unavailable, alternative ways to estimate it with a precision level compatible with the conceptual design phase shall be found. The P3-T3 method, as well as the FF method, can be employed to perform a Landing-Take-Off (LTO) emissions assessment by referencing the four throttle conditions outlined in Ref. [27] for the LTO cycle. The P3-T3 method is highly versatile and can therefore serve as an excellent tool for estimating NO_x emissions, even in the case of high-speed hydrogen-fueled aircraft, as documented in the literature [28] for an Air Turbo-Rocket Engine concept using hydrogen.

2.2. Fuel-flow method

The fuel-flow methods are developed starting from the P3-T3 method, with the intent of using only non-proprietary engine information, even if at the cost of the prediction accuracy. The main parameter considered by these prediction methods is the fuel flow, which represents the engine power setting and it can be retrieved from the user manual of the engine under study. In addition, these methods take into account the effect of ambient pressure and temperature, humidity, and Mach number. Three fuel-flow methods are presented in the literature: the Boeing Fuel-Flow Method 2 developed by Boeing (BFFM2) [29] and its applications [30,31] and the sustainable supersonic fuel-flow method [32]. This family of methods can be very useful for a preliminary estimation of the emissions even if the achievable accuracy is lower than those attainable from P3-T3 formulations. The variations of the fuel-flow method differ only in the introduced coefficients in the mathematical formulations. Therefore, it is decided to refer only to the BFFM2 below, as it is more commonly used in literature. The BFFM2 is selected as the baseline for the proposed update methodology for adapting to the estimation of NO_x for high-speed aircraft powered by hydrogen, similarly to what was proposed in Ref. [32] for a supersonic speed regime scenario and the use of Sustainable Aviation Fuel (SAF). Similar to the P3T3 method, the $EINO_{xFL}$ is derived from a correction of the $EINO_{xSL}$. However, for the BFFM2 method, this correction is performed based on the profiles of environmental conditions, the fuel flow profile W_f, and the Humidity Factor H. Unlike the P3-T3 method, the BFFM2 involves an additional intermediate fitting step concerning the fuel flow parameter. To derive this parameter under SL conditions from that under FL conditions, a mathematical formulation is provided which includes the Mach number. Although the fuel flow parameter is not directly included in the final mathematical formulation of the method used for evaluating $EINO_{xFL}$, it serves as the parameter based on which $EINO_{xSL}$ are plotted and interpolated. These interpolated values are then used for environmental correction, leading to $EINO_{xFL}$. The mathematical formulations prescribed by the FF method to estimate the fuel flow parameter under sea-level conditions, and consequently the produced $EINO_x$, are provided in Eqs. (3)–(6). The complete procedure for applying the original BFFM2 is documented in the literature [29] and includes an additional interpolation step compared to the P3T3 method.

$$w_{fSL} = w_{fFL}\frac{\theta_{amb}^{a}}{\delta_{amb}^{b}}\exp\left(c^{*}M^{d}\right) \quad (3)$$

$$\theta_{amb} = T_{amb}[K]/288.15 \quad (4)$$

$$\delta_{amb} = p_{amb}[Pa]/101325 \quad (5)$$

$$EINO_{xFL} = EINO_{xSL}\left(\frac{\delta_{amb}^{d}}{\theta_{amb}^{e}}\right)^{f}\exp(H) \quad (6)$$

where w_f is the fuel flow, H is the humidity factor introduced earlier for the P3-T3 method, and the parameters δ and θ represent the pressure and temperature ratios of environmental conditions (T_{amb}, p_{amb}) at varying altitudes to those under standard sea level conditions. Similar to the P3-T3 method, it is possible to use exponent coefficients specifically tailored for the engine under study, although the original formulation of the method prescribes the following values: d = 1.02, e = 3.3, f = 0.5.

3. Case study: Synergetic Air Breathing Rocket Engine fueled with hydrogen

This section provides an overview of the Skylon Reusable Launch Vehicle (RLV), a horizontal take-off and landing (HTOL) spaceplane developed by Reaction Engines Limited since 2009 to address the challenges of sustainable access to space [33]. Designed for Single-Stage-To-Orbit (SSTO) missions, Skylon operates like a conventional aircraft, taking off and landing horizontally, which simplifies its operational logistics and reduces the costs associated with dedicated launch facilities. The Skylon utilizes the Synergistic Air-Breathing Rocket Engine (SABRE) technology, a combined-cycle engine capable of both air-breathing and rocket modes throughout the mission. The SABRE engine operates initially as an air-breathing engine, using hydrogen fuel and atmospheric air up to an altitude of 25 km and speeds reaching Mach 5. Beyond this point, the engine transitions to rocket mode, switching to liquid oxygen (LO_X) for combustion, enabling the ascent to low Earth orbit. This dual-mode operation allows for a reduction in onboard propellant, increasing the payload capacity. This paper focuses on the air-breathing mode of the SABRE engine. In Fig. 1, the mass flows of the gases managed by the SABRE engine during the air-breathing phase and the Skylon mission profile are shown as a function of Mach. In air-breathing mode, SABRE employs a deeply precooled combined cycle, using helium for thermal management. Incoming air is cooled by helium in the PreCooler (PC) before compression in the Air Compressor (AC). The airflow then splits, with portions directed to the PreBurner (PB) and the main Combustion Chamber (CC) for staged combustion. The helium cycle regenerates heat from the initial combustion, heating the stored liquid hydrogen and powering the air compressor. This design maximizes efficiency and thrust during air-breathing mode, producing significant values of specific impulse, enabling efficient operation at high speeds without performance degradation [33–35]. The SABRE engine innovative architecture offers a high thrust-to-weight ratio, moderate specific fuel consumption during air-breathing mode, and optimal performance during the rocket phase, making it the best candidate for efficient and reusable space access.

3.1. State-of-the-art in propulsion and emission modeling

The SABRE propulsive system and the Skylon SSTO represent cutting-edge advancements in sustainable space access. However, publicly available data on the thermodynamic evolution of gases within the engine and resulting chemical emissions is minimal. Due to the absence of certified propulsive and emissive databases specific to the SABRE engine, simplified yet accurate models are employed to obtain necessary input data for developing new analytical formulations to estimate NO_x emissions from this high-speed hydrogen-fueled engine concept. During the state-of-the-art analysis on available data and models for the SABRE, two existing propulsion and emission models were selected as the starting point for refinement and optimization [36,37]. The reference propulsion model [36] outlined a strategy for the thermodynamic and propulsion modeling of the main air cycle of the engine operating in air-breathing mode. Building upon this model, several upgrades are implemented, allowing for a more precise estimation of the temperature and pressure values of the flows entering the mixers preceding the preburner and the main combustion chamber. These temperature and pressure data sets are then utilized to evaluate the mass fractions of species present in the exhaust gases of the two combustion stages of the SABRE using dedicated software, and consequently, to assess its $EINO_x$ using the same strategy proposed by the reference emissions model [37]. The engine consists of four thrust chambers, two preburner-reheater units, two hydrogen turbo-pumps, two regenerators, and two helium circulators, each driven by a hydrogen turbine. Therefore, the engine model can be effectively scaled down to one-quarter size to simplify the analysis. Assumptions include no incoming air to the ramjet burners throughout the mission profile and maintaining nominal pressure recovery at the intake while ensuring the air compressor matches the required mass flow. Fig. 2 illustrates the representative propulsion scheme of the propulsion model [36], depicting two distinct combined thermodynamic cycles.

As depicted in the propulsion schematic shown in Fig. 2, the SABRE engine encompasses two combined thermodynamic cycles: the complete air cycle and the regenerative helium cycle. The reference model [36] primarily focuses on the complete air cycle, tracing the path of the airflow entering the engine through the intake. Upon intake, the airflow is cooled by a cold helium stream within the precooler (PC), and then compressed in the air compressor (AC). Subsequently, the airflow splits into two streams at the PB-CC node, regulating the airflow directed to the engine two combustion stages. One stream undergoes rich fuel combustion with hydrogen in the PB, where exhaust gases exchange heat with helium before rejoining the remaining airflow upstream of the main combustion chamber (CC). Here, combustion concludes with the still fuel-rich mixture from the PB. The total exhaust gas flow from the CC then expands through a nozzle. The Matlab propulsion model [36] does not incorporate the study and implementation of the helium auxiliary thermodynamic cycle. The regenerative helium cycle, designed to ensure thermal balance among gas flows in the engine, is particularly significant for deeply precooled combined cycles like the SABRE. Therefore, integrating this regenerative cycle into the main model is essential for enhancing its reliability and thus the accuracy of the resulting data. Additionally, the model employs a conventional approach to simulate the SABRE, modelling the combustion processes under isobaric and isochoric stoichiometric conditions. While this

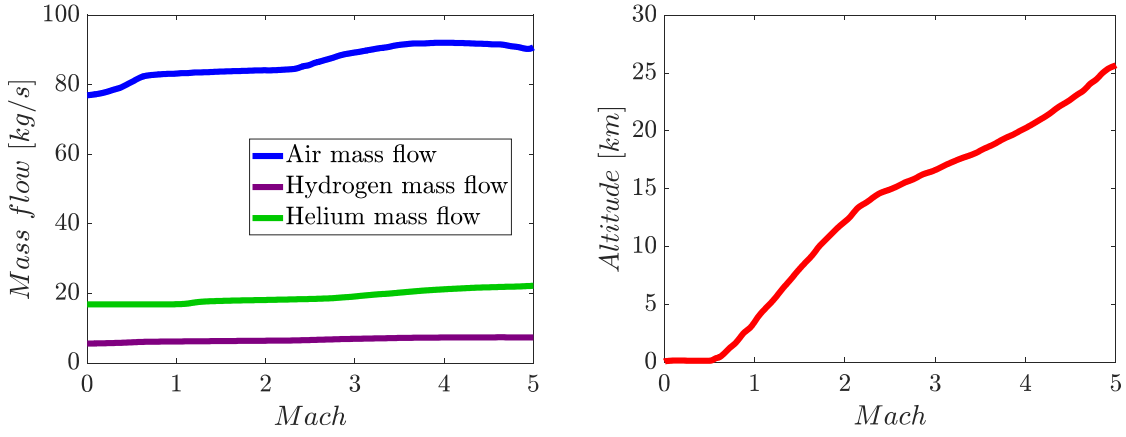

Fig. 1. SABRE engine mass flows and Skylon mission profile, as a function of Mach number.

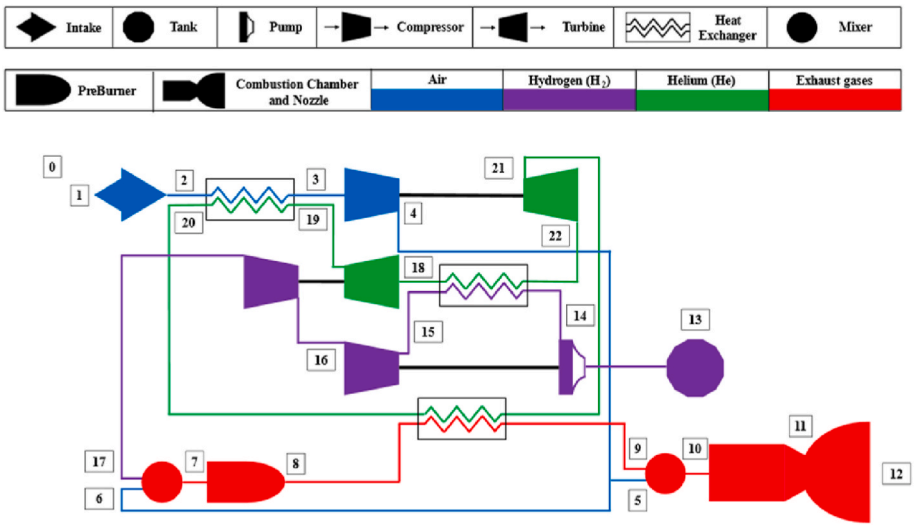

Fig. 2. Propulsion scheme of the SABRE engine from the reference propulsion model [36].

method yields reasonably accurate results, significant improvements can be achieved by integrating specialized software to address thermodynamic balance and equilibrium issues. Indeed, although the assumption of stoichiometric combustion is widely used during the conceptual design phase for preliminary combustion modeling, it fails to represent the highly fuel-rich conditions expected in the SABRE combustion process. Furthermore, dedicated software can enhance the accuracy of the mixing processes modelling and simplify the evaluation of gas thermodynamic characteristics. With these areas identified for potential refinement to advance the sophistication of SABRE propulsion model, the actual update of the model follows the approach outlined in Section 4.

Regarding the engine emission modelling, a previous study by the authors [37] serves as a reference. The approach involves utilizing the propulsive database generated from the model [36] to simulate mixing and combustion processes using specialized software. Specifically, Cantera, an open-source software for 0D/1D mathematical-chemical modelling, is employed via its Python interface. Cantera conducts 0D time-dependent simulations of homogeneous, isochoric, and adiabatic batch reactors with premixed gaseous reacting hydrogen/oxygen mixtures. For this purpose, the kinetic mechanism Z24_NOx20 developed by the Swedish Defence Research Agency FOI modelling group was effectively utilized [37]. The Z24_NOx_20 chemical kinetic mechanism is part of a suite of mechanisms used to model combustion processes and the formation of nitrogen oxides (NO_x), in hydrogen-rich combustion systems specifically. This mechanism is designed to simulate various chemical reactions that lead to the production of NO_x during H_2-Air combustion, including the thermal NO_x formation via the extended Zeldovich mechanism, as well as other less common pathways such as the NNH route and the prompt NO_x mechanism, which are more relevant in rich combustion conditions. The Z24_NOx_20 mechanism includes detailed reactions between nitrogen, oxygen, and hydrogen species, with a particular focus on the formation of NO_x under high-temperature combustion conditions (above 1700 K), incorporating results from low and high pressure experiments, and covering a wide range of equivalence ratios. The specific use of species like NNH, a key intermediate, reflects a deeper understanding of NO_x formation over a wider range of temperatures and residence times. For this reason, this mechanism is particularly suitable for estimating emissions and products resulting from the combustion of hydrogen and syngas [38,39]. The preburner combustion modelling was conducted under isobaric conditions, while the 0D simulations for the main combustion chamber assumed isochoric conditions. Additionally, the composition of the exhaust gases leaving the preburner was used as input for the main combustion chamber after mixing with the additional air stream from the intake. The required input data for the software included pressure values at the inlets of the two combustion stages and temperatures of the flows at the mixer inlets. The outputs provided temperature values of the flows exiting the mixers and the temperature and mass fractions of species present in the chamber at the end of combustion. Once the gas composition entering and leaving the main combustion chamber is known, the NO_x Emission Indices ($EINO_x$) can be calculated. Specifically, these indices were evaluated for each Mach condition based on the mass fraction of H_2 injected into the combustion chamber at the start of the simulation and the mass fractions of NO and H_2 at the end of combustion. The relationship for calculating the EINO in [g_{NO}/kg_{H2}] based on the mass fractions (Y) of NO and H_2 is provided in Eq. (7).

$$EINO = 1000 * \frac{Y_{NO}}{Y_{H2inj} - Y_{H2out}} \tag{7}$$

where Y_{NO}, Y_{H2inj} and Y_{H2out} are the mass fractions of NO produced during combustion, injected fuel H_2 in the chamber, and unburned H_2, respectively. It's important to note that for SABRE, and more broadly for hydrogen-air combustion, the mass fraction of NO produced during combustion is predominantly used for estimating the engine NO_x Emission Indices, as it is several orders of magnitude higher than other NO_x compounds. Considering this emission modelling approach, what requires updating is not the modelling technique itself, which is considered accurate for conceptual design, but rather the emissive database resulting from the application of this technique based on the propulsion database formulated using model [36].

4. H2-P3T3 and H2-BFFM2: methodology and novel formulations

A step-by-step methodology is proposed to update the classical formulations of the P3-T3 and the FF methods. Specifically, novel mathematical formulations are derived for estimating the NO_x emissions produced by the hydrogen-fueled SABRE engine during its air-breathing phase, starting from the original formulations of two selected emission estimation methods, as documented in Section 4.1, namely the P3-T3 and the BFFM2. The initial step of the adopted methodology involves recalculating the propulsive and emissive databases of the engine. The reference propulsion and emission models are updated based on the refinement criteria identified in Section 3. In Sections 4.2 and 4.3 the new mathematical formulations H2-P3T3 and H2-FF for estimating $EINO_x$ are described, focusing on the correlation logic behind the

introduction of the new parameters compared to the original P3-T3 and BFFM2. The recalculated $EINO_x$ from the updated emission database are then compared with those predicted by the novel H2-P3T3 and H2-FFM formulations in Section 5, and the results are discussed in terms of the accuracy of the new relationships.

4.1. Methodology for updating the emissions estimation methods

The proposed methodology for deriving new mathematical formulations for estimating the $EINO_x$ from the SABRE engine involves several key steps and considerations, summarized in the block diagram shown in Fig. 3.

4.1.1. Update of the propulsion model

Developing a more reliable propulsion model, accurately representing the actual functioning and performance of the studied engine, is crucial to achieve the most accurate estimation possible of its emissions during the conceptual design phase. In fact, the Propulsive Database shall be then used as input for the chemical-kinetic modelling of the engine, and consequently for the development of the Emissive Database. This database shall include mass fractions of chemical species in the inlet and outlet flows of the engine combustion stages, along with the resulting $EINO_x$ evaluated with Eq. (7). In details, the SABRE engine model already available in literature [36] is updated by:

(i) *integrating the regenerative thermodynamic cycle of helium*. While in the original model [36] the Helium properties were assumed constant and fixed at their mean value within the cycle, this work considers the thermodynamic evolution of helium within its regenerative closed-loop. This is facilitated by utilizing the Matlab interface of the Cantera software, that enables the assessment of specific properties of the gas at each intermediate temperature and pressure conditions within each component of the cycle. Essential inputs for the cycle modelling, i.e. the helium flow rate data and helium inlet pressure profile to the helium turbine are obtained from Ref. [40].

(ii) *allowing for the simulation of thermodynamic equilibrium in the combustion chambers using Cantera in Matlab*. The simulation of chemical equilibrium conditions during fuel-rich combustion of the SABRE engine, performed using Cantera in Matlab, allows for the refinement of the original combustion modeling strategy, which was initially based on the assumption of stoichiometric conditions. Furthermore, the use of Cantera for combustion modeling enables the preliminary estimation of $EINO_x$ within the propulsion model by leveraging the mass fractions of species when chemical equilibrium is reached. It is worth noticing that, while these $EINO_x$ are not suitable as references due to being less reliable compared to those resulting from 0D chemical-kinetic simulations executable with Cantera via Python, they nonetheless provide an estimation of the profile in NO_x formation in the combustion chamber across varying Mach numbers.

(iii) *integrating the results of the mixing processes modelling using Cantera in Python*. The Cantera Python modelling takes as input the pressure and temperature data of the incoming flows to the mixers, derived from the developed propulsion model, and returns the same parameters referred to the mixed state. These parameters are then subsequently integrated into the Matlab model to continue with the cycle modelling.

After implementing the described updates to the reference propulsion model [36], it is possible to evaluate the engine performances. The specific thrust and specific impulse resulting from the performance analysis are plotted and compared with the corresponding reference data from the high-level simulation of the SABRE [40] conducted using the EcosimPro framework in Fig. 4.

4.1.2. Update of the chemical emissions model

Regarding the chemical-emissive modelling of the engine, Cantera via Python interface and the kinetic mechanism Z24_NOx20 are used as suggested in Ref. [37]. For the combustion processes, both the chemical equilibrium of the mixed gases and their time-dependent chemical-kinetic evolution within ideal reactors are simulated. Specifically, isobaric combustion conditions are simulated for the preburner, while isochoric conditions are considered for the main combustion chamber. Regarding the PB exhaust gases, the attainment of chemical equilibrium conditions is assumed. The composition and properties of the exhaust gases are evaluated applying the principle of Gibbs free energy minimization to the system. Similarly, the main combustion chamber (CC) is initially modeled based on Gibbs free energy minimization, thus assuming chemical equilibrium conditions. In the chemical equilibrium calculation, Cantera searches for the final composition of a combusted gas mixture that minimizes the Gibbs free energy, under constraints of

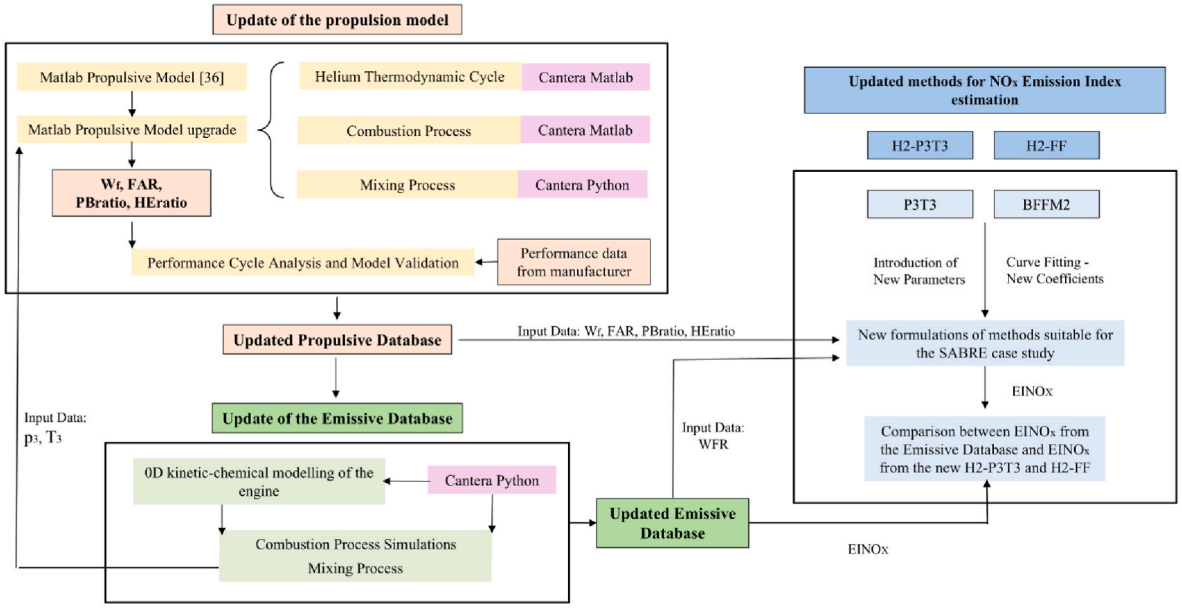

Fig. 3. Workflow for updating NO_x emission estimation P3T3 and Fuel-Flow Methods.

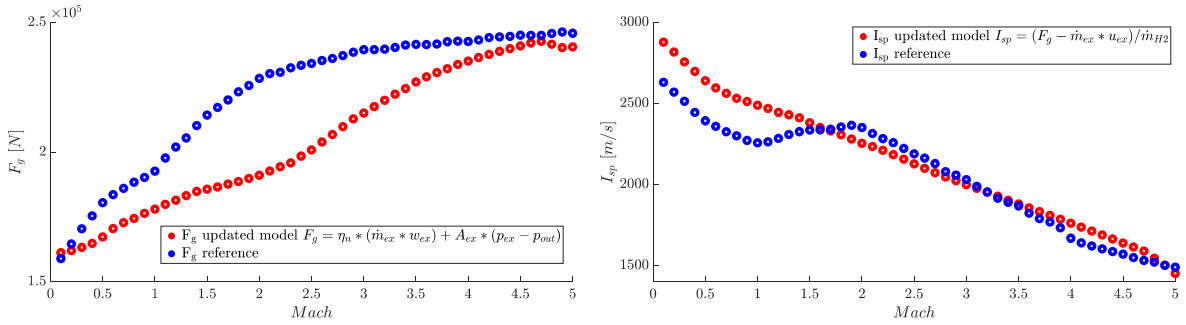

Fig. 4. SABRE propulsive performances of the updated propulsion model compared to the reference performances [40].

mass, energy, and momentum conservation. This approach considers the chemical reactions to be infinitely fast and assumes chemical equilibrium as the state in which the forward and reverse reactions are fully balanced. From the evaluated gas mixture composition in the main CC, a preliminary set of thermodynamic $EINO_x$ for SABRE was derived i.e., under chemical equilibrium conditions computed by minimizing the system Gibbs free energy. However, to gain further insights into the combustion process in the main CC, time-dependent chemical-kinetic simulations of the gas evolution during combustion are conducted too. Starting from the temporal evolution profiles of species mass fractions in the combustion chamber, obtained from kinetic simulations, the kinetic $EINO_x$ were evaluated at the simulation end time. In kinetic calculations, differential equations that describe the temporal evolution of chemical species concentrations are solved, accounting for reaction rates, mass and heat transfer dynamics. Unlike the chemical equilibrium calculation, the process is not instantaneous: it analyzes how the system approaches equilibrium over time, considering slow reactions, reactive intermediates, and reaction pathways. Thus, the kinetic $EINO_x$ represent a more accurate evolution of gases within the combustor over time and better capture the chemical-kinetic dynamics of the hydrogen oxidation process. Therefore, these $EINO_x$ are assumed as reference $EINO_x$ for updating the P3-T3 and FF methods for NO_x estimation. Fig. 5 provides a comparison between the $EINO_x$ values from the original [37] and updated emissive databases. For the purpose of this study, the emissive database is massively expanded compared to that reported in Ref. [37] by studying 50 different Mach conditions equally spaced between Mach 0 and Mach 5.

4.1.3. Update of the methods formulations

The final step of the methodology involves modifying the classical formulations of the P3-T3 and the Fuel-Flow methods to extend their applicability to the characteristics of the case study. According to the authors, the best approach to adjust the traditional analytical formulations of the $EINO_x$ estimation methods to high-speed, hydrogen-fueled case studies is to enhance the already existing formulations by integrating novel parameters which closely correlate with NO_x emissions indices along the mission profile. Therefore, this adaptation and enhancement process from the original P3-T3 and BFFM2 is carried out through two sequential modifications: (i) the inclusion of new parameters in the form of ratios between FL and SL conditions, coupled with (ii) the curve fitting of the resulting mathematical formulations based on a subset of $EINO_x$ under flight level conditions from the emissive database. The parameters selected to be introduced into the new formulations are the result of the correlations analysis assessing the links between the chemical-thermodynamic variables and the processes of NO_x emissions formation within the engine. Indeed, it is reasonable to assume that the best approach to adjust the traditional analytical formulations of the $EINO_x$ estimation methods to the high-speed, hydrogen-fueled case study is to integrate parameters into the formulations whose profiles during the mission closely correlate with those of the NO_x emissions indices to be estimated.

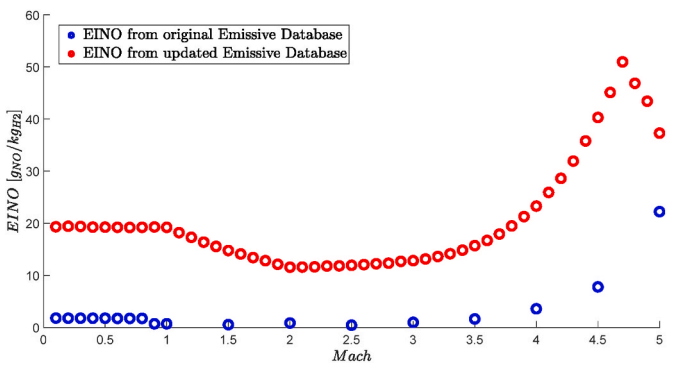

Fig. 5. Comparison between EINO from the original [37] and updated emissive databases.

Notably, the primary correlation observed for the SABRE is between the NO_x produced and the Flame Temperature (FT) in the combustion chamber. Indeed, an increase in the temperature reached in the combustion chamber results in an increase in NO_x produced by the engine. However, FT is proprietary data that is challenging to estimate in conceptual design. For this reason, parameters easily estimable yet significantly influencing flame temperature were selected for adapting the $EINO_x$ estimation methods to the case study. Specifically,

(i) the Mach parameter was introduced to account for the effects of high speed on the temperature and pressure of the incoming airflow through the engine intake, and consequently, on the temperature achieved within the combustion chamber;
(ii) the FAR ratio was introduced to consider the decrease in temperature reached during fuel-rich combustion as a function of the increase in the fuel percentage. Indeed, an increase in the FAR leads to a higher fraction of H_2 at the combustion chamber inlet, causing a deviation from the stoichiometric combustion condition and consequently resulting in a decrease in the temperature reached within the combustion chamber;
(iii) the PBratio parameter was introduced, i.e. the ratio between the air flows directed to the PreBurner and the main combustion chamber following the split downstream of the air compressor. This parameter was selected to account for the decrease in temperature reached in the combustion chamber due to the segmented combustion of the SABRE;
(iv) the Water-to-Fuel Ratio (WFR), closely related and with the same trend as the PBratio, was introduced to consider both the effect of the decreasing temperature reached during combustion due to the presence of a water fraction at the inlet of the main combustion chamber resulting from the combustion stage in the PB and the chemical-kinetic influence of the hydrogen oxidation process. Water vapor affects NO_x formation through three primary mechanisms. As reported in Ref. [41], water vapor dilution of the combustion mixture reduces NO_x emissions in premixed

flames by lowering the flame temperature, creating an oxygen deficiency, and through chemical action;

(v) the HEratio parameter was introduced to consider the increase in the temperature reached in the chamber as a function of the thermal power that the engine must manage through the helium regenerative cycle.

These new parameters, which vary along the SABRE mission profile, were integrated into the new formulations of the H2-BFFM2 and H2-P3-T3 methods. They were expressed as ratios between conditions at Flight Level (FL) and Sea Level (SL), ensuring continuity with the original methods. Different combinations of parameters resulted in different curve fitting optimization coefficients and thus in resulting errors for the modified formulations, evaluated against the reference $EINO_x$ from the emissive database.

4.2. H2-P3T3 - new formulations of the P3-T3 method

Considering the absence of certified standards for the inlet temperature to the main combustion chamber (T_3) and $EINO_x$ values at sea level conditions for the SABRE, the steps required for the application of the updated H2-P3T3 formulations to the case study can be summarized in the following list:

1. As the initial step, it is necessary to construct fits based on the known data under sea level conditions collected in the propulsive and emissive databases, in order to study their trend with varying flight conditions. Given the absence of standardized sea level reference values, linear fits are created by interpolating the first 4 values of the different parameters tabulated in the respective databases as a function of Mach, corresponding to Mach conditions ranging from 0.1 to 0.4, representing the engine operation at sea level altitudes. The parameters p_{3SL}, FAR_{SL}, $PBratio_{SL}$, WFR_{SL}, $HEratio_{SL}$, and $EINO_{SL}$ obtained from the updated propulsive and emissive databases are interpolated as functions of T_3. For the SABRE engine, reference sea level conditions as a function of the main combustor inlet temperature can be mathematically expressed using the fitting functions shown in Fig. 6, in comparison to the values under sea level conditions from the updated databases. For the sake of simplicity, given the limited sea level data available from the two databases, the most commonly used interpolation method was linear polynomial interpolation. However, for FAR and HEratio, exponential interpolation was preferred to avoid encountering unreasonable values for these parameters as T_3 increases. From these fittings, it is possible to compute the ratios between sea level (SL) and flight level (FL) conditions, also utilizing the databases for the values corresponding to the latter.
2. Once the ratios are determined, it is possible to evaluate the $EINO_{FL}$ starting from the $EINO_{SL}$, employing one of the formulations presented in Eqs. (8)–(11). The exponent coefficients in the new formulations are optimized using a subset of $EINO_x$ from the updated emissive database. Specifically, data corresponding to 32 of the 50 Mach conditions studied are used as references for optimizing the exponents, while the remaining 18 conditions, corresponding to those in the original emissive database (Fig. 5), are utilized to test the accuracy of the new formulations. For each new formulation, the multiplicative coefficient k and the exponent coefficients are optimized starting from the initial guess of the original P3-T3 method, ensuring the best possible estimation of the reference $EINO_{FL}$.

$$EINO_{FL} = k * EINO_{SL} \left(\frac{p_{3FL}}{p_{3SL}}\right)^{a} \left(\frac{FAR_{FL}}{FAR_{SL}}\right)^{b} M^{c} * \exp(H) \tag{8}$$

$$EINO_{FL} = k * EINO_{SL} \left(\frac{p_{3FL}}{p_{3SL}}\right)^{a} \left(\frac{FAR_{FL}}{FAR_{SL}}\right)^{b} * (ratio1)^{i} * M^{c} * \exp(H) \tag{9}$$

$$EINO_{FL} = k * EINO_{SL} \left(\frac{p_{3FL}}{p_{3SL}}\right)^{a} \left(\frac{FAR_{FL}}{FAR_{SL}}\right)^{b} * (ratio1)^{p} * (ratio2)^{q} * M^{c} * \exp(H) \tag{10}$$

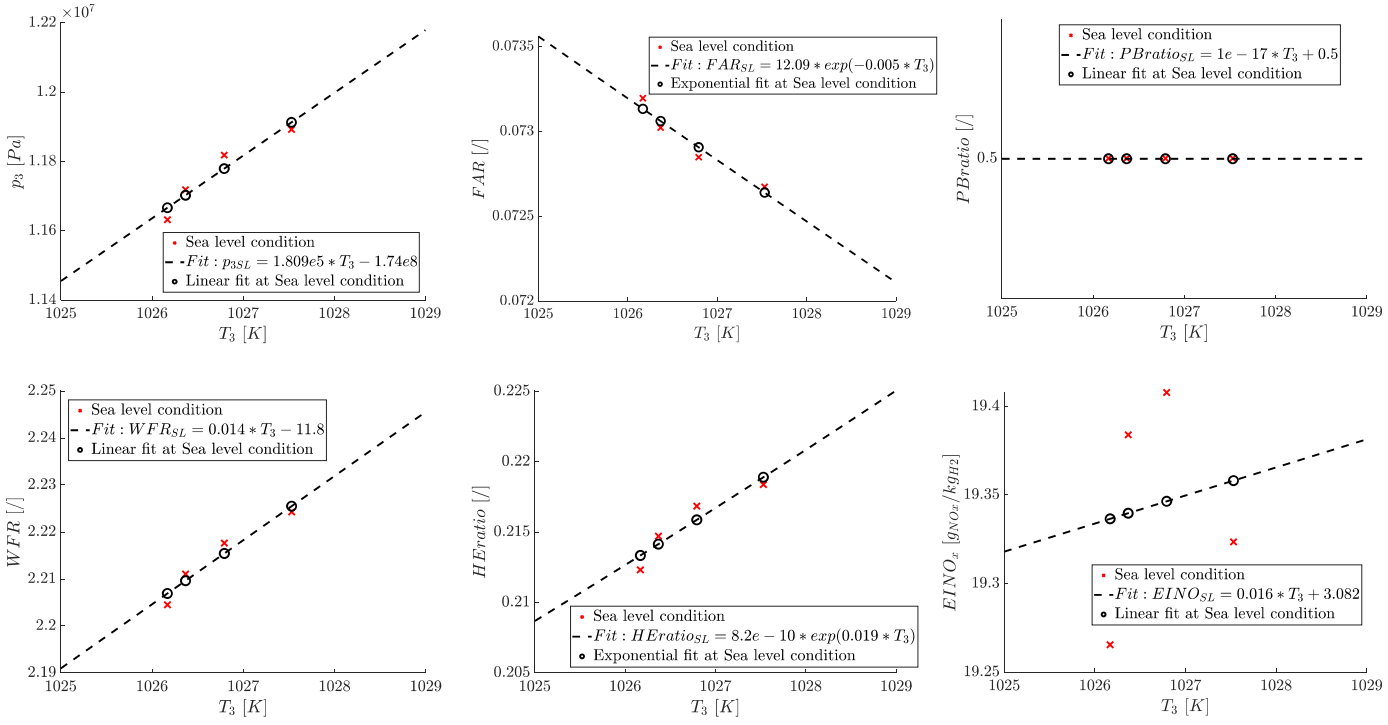

Fig. 6. Sea level conditions as a function of the combustion inlet temperature, in terms of a) pressure at the inlet of the combustion chamber, b) Fuel to Air Ratio, c) air mass flow rate i.e., PB_{ratio}, d) Water to Fuel Ratio at the inlet of the combustion chamber, e) He-air mass flow rate i.e., HE_{ratio}, f) NO Emission Index.

$$EINO_{FL} = k^{*}EINO_{X\ SL}\left(\frac{p_{3FL}}{p_{3SL}}\right)^{a}\left(\frac{FAR_{FL}}{FAR_{SL}}\right)^{b}\left(\frac{PB_{ratioFL}}{PB_{ratioSL}}\right)^{r}\left(\frac{WFR_{FL}}{WFR_{SL}}\right)^{s}\left(\frac{HE_{ratioFL}}{HE_{ratioSL}}\right)^{t} M_0^{c}\, e^{H} \quad (11)$$

where the parameters defined by the original P3-T3 formulation are the inlet pressure of the main combustion chamber (p_3) and the Fuel to Air Ratio (FAR), while the newly introduced parameters are the Mach number, the Water to Fuel Ratio (WFR), and the mass flow ratios PBratio and HEratio defined in Section 4.1.2. The subsequent steps consist of the progressive addition of one, two, or all of the ratios of the newly introduced parameters. In Eq. (11), all the ratios of the new parameters introduced can be observed, while in Eq. (9) and Eq. (10), the terms "ratio1″ and "ratio2″ are used to generalize the equations for all combinations of ratios. The optimized coefficients for each combination of introduced ratios, thus for each new formulation of the P3-T3 method, are reported in Tables 1 and 2. Please refer to the first column of the tables and to Eqs. (8)–(11) to identify the corresponding mathematical correlation for each table.

Overall, significant variations can be observed in the sign of the optimized exponents as the number of parameters and ratios introduced in the new formulations increases. This fluctuation in the behaviour of the coefficient exponents may be due to the purely mathematical optimization performed in Matlab, which disregards the physics and chemistry of the processes and bases the recalculation of these coefficients solely on the input data. Since the ratios between FL and SL conditions exhibit markedly different trends with respect to Mach, it is expected to obtain different optimized exponents for different combinations of these ratios. Indeed, the optimization process refers to a single set of $EINO_x$ for determining the best fit for all the new mathematical formulation, which nonetheless present different ratio values that are involved. Considering the most comprehensive formulation (see Eq. (11)), whose optimized coefficients are reported in Table 3, it is possible to derive some physical-chemical conclusions and justifications about these coefficients. Some of the parameters included in the new formulation, i.e., FAR and Heratio, provide mathematical contributions to the calculation of $EINO_x$ that are not consistent with the physical expectations derived from the correlation analysis. The mathematical contributions of the parameters are determined by the sign of their optimized exponents and their magnitude. These contributions and their justifications are thoroughly discussed by the authors in a previous publication [42].

4.3. H2-FF - new formulations of the FF method

Analogously to the process outlined for the new H2-P3T3 formulations, the step-by-step approach for the H2-FF method is explained below. Unlike the P3-T3 method, this update involved an additional optimization step concerning the coefficients in Eq. (3) used to evaluate the fuel flow at sea level conditions from the flight level conditions. Considering the absence of certified standards for fuel flow and $EINO_x$ values at sea level conditions for the SABRE, the steps required for the application of the updated H2-FFM formulations to the case study can be summarized according to the following list:

1. As a first step, it is necessary to derive the fuel flow values at sea level by applying the following correction to the fuel flow values in FL conditions. The relationships are the same employed in the original version of the fuel-flow method (sees Eq. (3), Eq. (4), and Eq. (5)). The trend of the fuel flow profile at sea level, evaluated using the classical formulation of the BFFM2, exhibits an exponential increase with rising Mach numbers, as depicted in Fig. 7. Consequently, an initial correction is undertaken by recalculating the exponents of the original mathematical formulation through Matlab curve fitting functionalities. This fit is depicted in Fig. 7 alongside the values of w_{fSL} from the propulsive database. Evaluating the value of this linear fit for each Mach condition from 0.1 to 5, it is possible to recalculate the exponents *a, b, c* and *d* using curve fitting. The original and updated exponents are listed in Table 4. The profile of w_{fSL} as a function of Mach resulting from the application of the w_{fSL} correction with the updated coefficients is presented in Fig. 7.
2. $EINO_{SL}$, FAR_{SL}, $PBratio_{SL}$, WFR_{SL}, and $HEratio_{SL}$ obtained from the updated propulsive and emissive databases for the first four Mach conditions are curve-fitted as a function of the corrected W_{fSL} from step 1. For the SABRE engine, reference sea level conditions as a function of the fuel flow at sea level, evaluated as in step 1, can be mathematically expressed using the fitting functions shown in Fig. 8, in comparison to the values under sea level conditions from the updated databases. Similarly to the P3-T3 method, due to the limited availability of sea level data from the two databases, linear polynomial interpolation was employed to construct these fits. From these fittings, it is possible to compute the ratios between sea level (SL) and flight level (FL) conditions, also utilizing the databases for the values corresponding to the latter.
3. Once the ratios are determined, it is possible to evaluate the $EINO_{FL}$ starting from the $EINO_{SL}$, employing one of the formulations reported in Eqs. (12) and (13). The exponent coefficients for the FF method are also updated using a reference subset of 32 $EINO_x$ from the updated emissive database.

$$EINO_{FL} = k^{*}EINO_{SL}\left(\frac{\delta_{amb}^{a}}{\theta_{amb}^{b}}\right)^{c} {}^{*}M^{d} {}^{*}\exp(H) \quad (12)$$

Table 1
$EINO_{FL} = f\,(EINO_{SL}, p_3, FAR, Mach, ratio1)$.

	k	a	b	c	i
Original $EINO_{FL} = f\,(EINO_{SL}, p_3)$	1.00	0.40	0.00	–	–
$EINO_{FL} = f\,(EINO_{SL}, p_3, FAR)$	1.00	3.26	3.32	–	–
$EINO_{FL} = f\,(EINO_{SL}, p_3, FAR, M)$	0.98	3.24	3.47	−0.14	–
$EINO_{FL} = f\,(EINO_{SL}, p_3, FAR, M, PB_{ratio})$	1.00	0.69	1.12	−0.37	−5.05
$EINO_{FL} = f\,(EINO_{SL}, p_3, FAR, M\ WFR)$	1.00	2.48	1.10	−0.39	−2.33
$EINO_{FL} = f\,(EINO_{SL}, p_3, FAR, M, HE_{ratio})$	0.78	1.78	15.36	−0.83	3.56

Table 2
$EINO_{FL} = f\,(EINO_{SL}, p_3, FAR, Mach, ratio1, ratio2)$.

	k	a	b	c	p	q
$EINO_{FL} = f\,(EINO_{SL}, p_3, FAR, M, PB_{ratio}, WFR)$	1.00	−3.31	3.80	0.04	−18.89	8.99
$EINO_{FL} = f\,(EINO_{SL}, p_3, FAR, M, PB_{ratio}, HE_{ratio})$	0.79	−1.58	−13.52	−0.48	−3.64	−11.51
$EINO_{FL} = f\,(EINO_{SL}, p_3, FAR, M, WFR, HE_{ratio})$	1.08	−3.55	0.62	−0.10	−2.82	4.89

Table 3
$EINO_{FL} = f\,(EINO_{SL}, p_3, FAR, Mach, PB_{ratio}, WFR, HE_{ratio})$.

k	a	b	c	r	s	t
1.04	−3.51	12.79	0.07	−19.56	11.40	2.11

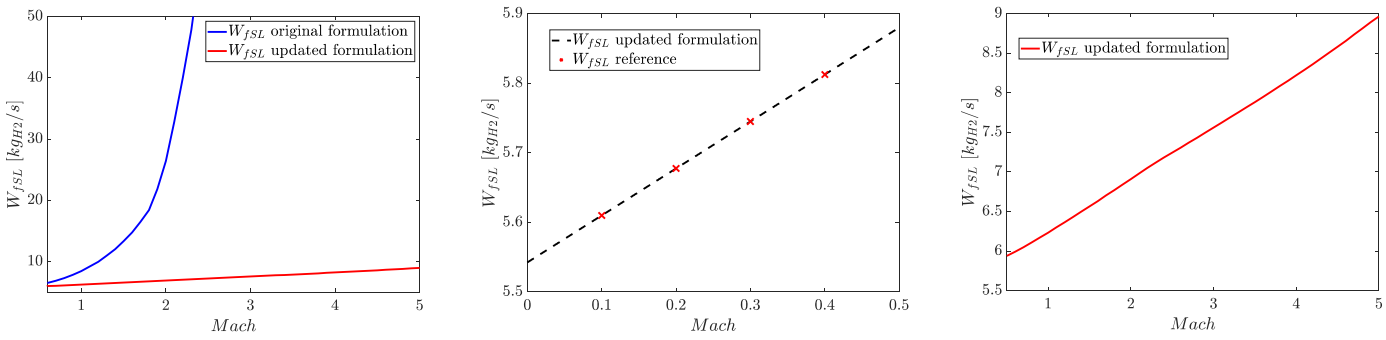

Fig. 7. w_{fSL} profile and linear fit as a function of Mach.

Table 4
Original and updated exponents for fuel flow correction.

	a	b	c	d
Original $w_{fSL} = f(\theta_{amb}, \delta_{amb}, M)$	3.8	1	0.2	2
Updated $w_{fSL} = f(\theta_{amb}, \delta_{amb}, M)$	0.0084	0.0207	0.0089	1.4917

$$EINO_{FL} = k^{*}EINO_{SL}\left(\frac{\delta^{a}_{amb}}{\theta^{b}_{amb}}\right)^{c} {}^{*}(ratio1)^{i} {}^{*}M^{d} {}^{*}\exp(H) \quad (13)$$

$$EINO_{FL} = k^{*}EINO_{SL}\left(\frac{\delta^{a}_{amb}}{\theta^{b}_{amb}}\right)^{c} {}^{*}(ratio1)^{p} {}^{*}(ratio2)^{q} {}^{*}M^{d} {}^{*}\exp(H) \quad (14)$$

where the parameters defined by the original FF formulation are the environmental pressure and temperature ratios δ and θ, while the newly introduced parameters are the Mach number, the Fuel to Air Ratio (FAR), the Water to Fuel Ratio (WFR), and the mass flow ratios PBratio and HEratio defined in Section 4.1.2. For each new formulation, the multiplicative coefficient k and the exponent coefficients are optimized starting from the initial guess of the original BFFM2 method, ensuring the best possible estimation of the reference $EINO_{FL}$. The optimized coefficients for each combination of introduced ratios, thus for each new formulation of the FF method, are reported in Tables 5 and 6. Please refer to the first column of the tables and to Eqs. (12)–(15) to identify the corresponding mathematical formulation for each table.

In contrast to the findings observed for the H2-P3T3 method,

$$EINO_{FL} = k^{*}EINO_{X\,SL}\left(\frac{\delta^{a}_{amb}}{\theta^{b}_{amb}}\right)^{c}\left(\frac{HE_{ratioFL}}{HE_{ratioSL}}\right)^{r}\left(\frac{WFR_{FL}}{WFR_{SL}}\right)^{s}\left(\frac{FAR_{FL}}{FAR_{SL}}\right)^{t}\left(\frac{PB_{ratioFL}}{PB_{ratioSL}}\right)^{u} M_0^{d}\, e^{H} \quad (15)$$

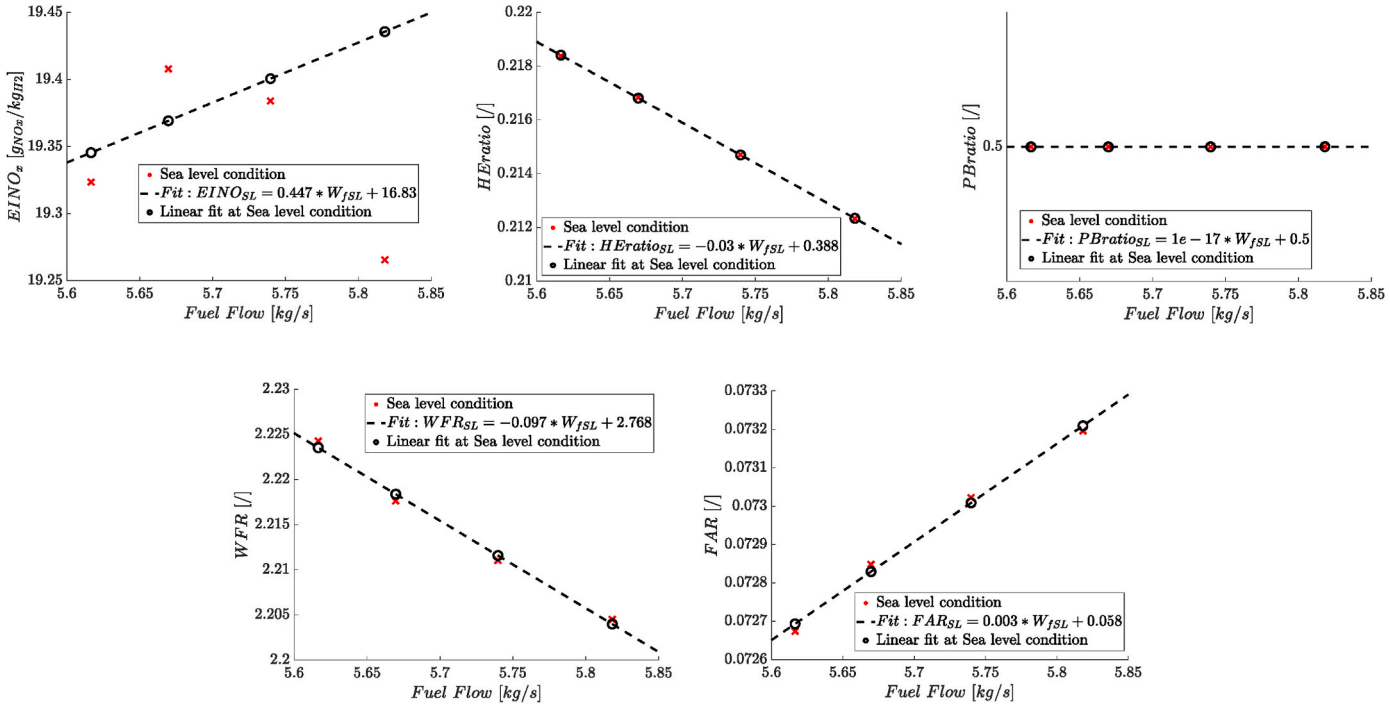

Fig. 8. Sea level conditions as a function of the combustion inlet temperature, in terms of a) NO Emission Index, b) He-air mass flow rate i.e., HE_{ratio}, c) air mass flow rate i.e., PB_{ratio}, d) Water to Fuel Ratio at the inlet of the combustion chamber, e) Fuel to Air Ratio.

Table 5
$EINO_{FL} = f$ ($EINO_{SL}$, δ_{amb}, θ_{amb}, Mach, ratio1).

	k	a	b	c	d	i
Original $EINO_{FL} = f$ ($EINO_{SL}$, δ_{amb}, θ_{amb})	1	1.02	3.3	0.5	–	–
$EINO_{FL} = f$ ($EINO_{SL}$, δ_{amb}, θ_{amb}, M)	0.94	0.27	2.40	−2.37	−0.09	–
$EINO_{FL} = f$ ($EINO_{SL}$, δ_{amb}, θ_{amb}, M, FAR)	1.00	0.30	2.73	−2.17	−0.06	0.47
$EINO_{FL} = f$ ($EINO_{SL}$, δ_{amb}, θ_{amb}, M, PB_{ratio})	1.00	0.23	2.17	−2.58	−0.06	−0.14
$EINO_{FL} = f$ ($EINO_{SL}$, δ_{amb}, θ_{amb}, M, WFR)	1.00	0.40	3.86	−1.52	−0.06	−0.16
$EINO_{FL} = f$ ($EINO_{SL}$, δ_{amb}, θ_{amb}, M, HE_{ratio})	1.00	0.39	3.86	−1.62	−0.08	0.15

Table 6
$EINO_{FL} = f$ ($EINO_{SL}$, δ_{amb}, θ_{amb}, Mach, ratio1, ratio2).

	k	a	b	c	d	p	q
$EINO_{FL} = f$ ($EINO_{SL}$, δ_{amb}, θ_{amb}, M, PB_{ratio}, FAR)	1.00	0.32	2.99	−1.88	−0.05	−0.12	0.08
$EINO_{FL} = f$ ($EINO_{SL}$, δ_{amb}, θ_{amb}, M, PB_{ratio}, WFR)	1.00	0.33	3.14	−1.82	−0.06	−0.14	−0.17
$EINO_{FL} = f$ ($EINO_{SL}$, δ_{amb}, θ_{amb}, M, PB_{ratio}, HE_{ratio})	1.00	0.11	0.77	0.99	−0.04	−1.62	1.52
$EINO_{FL} = f$ ($EINO_{SL}$, δ_{amb}, θ_{amb}, M, FAR, HE_{ratio})	1.00	0.31	3.02	−1.79	−0.05	0.08	0.10
$EINO_{FL} = f$ ($EINO_{SL}$, δ_{amb}, θ_{amb}, M, FAR, WFR)	1.00	0.04	0.74	−2.73	−0.05	0.68	−0.83
$EINO_{FL} = f$ ($EINO_{SL}$, δ_{amb}, θ_{amb}, M, HE_{ratio}, WFR)	1.00	0.55	5.47	−1.10	−0.09	−0.09	−0.22

Table 7
$EINO_{FL} = f$ ($EINO_{SL}$, δ_{amb}, θ_{amb}, Mach, HE_{ratio}, WFR, FAR, PB_{ratio}).

k	a	b	c	d	r	s	t	u
1.00	0.21	1.98	−1.88	−0.17	0.40	−0.99	−0.02	−0.82

regarding the new formulations of the FF method, a relatively stable trend in the optimized exponents emerges as the number of introduced parameters and ratios increases. With the addition of each new ratio, the optimized coefficients for the ratios evaluated in the previous formulation are therefore validated by the non-oscillation of the recalculated coefficients. Considering the most comprehensive formulation (see Eq. (15)), whose optimized coefficients are detailed in Table 7, it is possible to derive physical-chemical insights and justifications regarding these coefficients. Similarly to H2-P3T3, some of the parameters included in the H2-FF new formulation, i.e., FAR, Mach, and ambient pressure ratio, provide mathematical contributions to the calculation of $EINO_x$ that are not consistent with the physical expectations derived from the correlation analysis. These contributions and their justifications are thoroughly discussed by the authors in a previous publication [43].

5. Result and discussion

This section reports the results of the application of the newly developed formulations to the SABRE engine case study. The more comprehensive formulations of the H2-P3T3 and H2-FF methods, applied to the SABRE engine, return the $EINO_{FL}$ trends shown in Fig. 9, compared with the $EINO_{FL}$ values from the updated emissive database. These formulations, which incorporate all the newly introduced parameters, proved to be the most accurate in estimating NO_x emissions indices for both the H2-P3T3 and H2-FF methods.

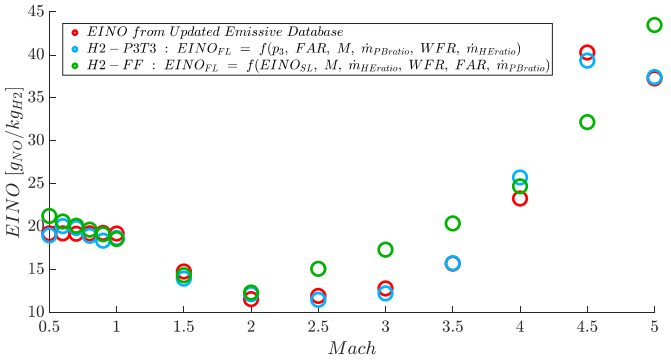

Fig. 9. $EINO_{FL}$ from (i) Updated Emissive Database, (ii) H2-P3T3 most comprehensive formulation, (iii) H2-FF most comprehensive formulation.

5.1. H2-P3T3 formulations for the SABRE engine

Finally, it is possible to graphically compare the $EINO_{FL}$ evaluated with the different formulations to the reference $EINO_{FL}$ from the emissive database obtained through 0D chemical-kinetic simulations by deriving the corresponding absolute and relative estimation errors. Fig. 10 compares the predictions from the various H2-P3T3 formulations reported in Table 1.

Regarding the more comprehensive formulations derived for the P3-T3 method, Fig. 11 compares the predictions from the various formulations reported in Tables 2 and 3, showing the evaluated emissions estimation errors with reference to the $EINO_{FL}$ trend from the updated emissive database.

5.2. H2-FFM formulations for the SABRE engine

Finally, Fig. 12 compares the predictions from the various H2-FF formulations reported in Table 5, specifically the formulations that include only a single additional parameter. Similarly to what was done for the H2-P3T3, the absolute and relative emissions estimation errors of the novel H2-FF formulations were evaluated against the reference $EINO_{FL}$ trend from the emissions database.

The novel H2-FF formulations result in significantly larger estimation errors compared to those from the novel H2-P3T3 formulation. This error trend highlights the inherently higher accuracy of the P3-T3 method compared to the FF method, as already documented in the literature regarding the application of the original formulations of these methods in subsonic applications using conventional fuels. The superior accuracy of the P3-T3 method relative to the FF method, also observed in the updated H2-P3T3 and H2-FF formulations, can be attributed to the different nature of the parameters involved in the two estimation methodologies, proprietary and non-proprietary. In the P3-T3 method, thermodynamic variables such as the pressure and temperature at the inlet of the combustion chamber are employed, which have a direct and predominant impact on the profiling of NO_x emissions for the engine under study. Conversely, in the FF method, the fundamental parameter for interpolation is the fuel flow. While fuel flow is indeed an important factor in emission studies, it remains an engine-level parameter. To minimize emission estimation errors, it is therefore preferable to adopt the P3-T3 methodology, which relies on parameters that more

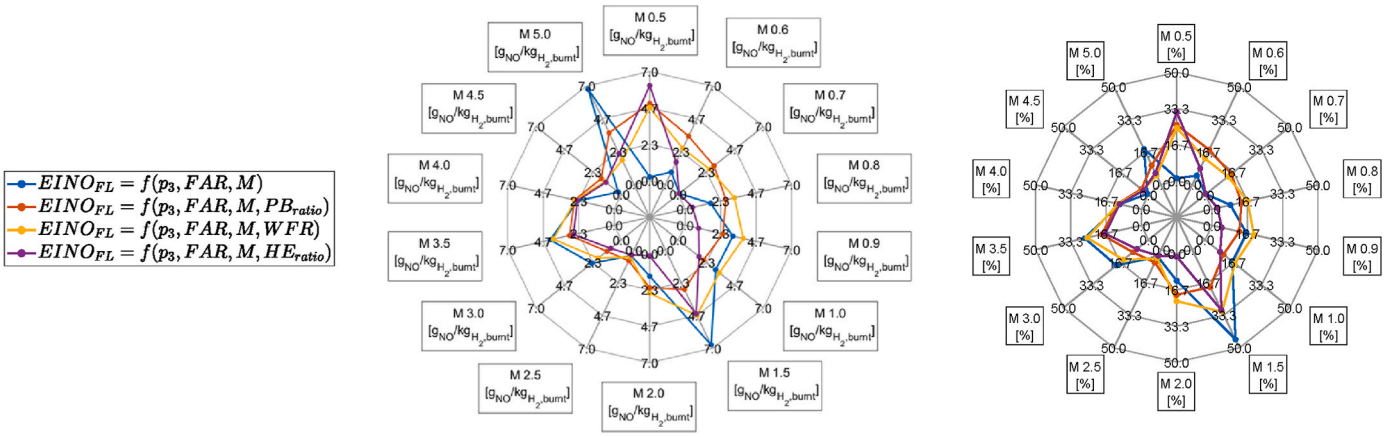

Fig. 10. Novel H2-P3T3 estimation errors evaluated for 14 Mach conditions ranging from 0.5 to 5, compared to the reference EINO from the updated emissions database: $EINO_{FL}$ absolute estimation errors [$g_{NO}/kg_{H2burnt}$] (left) and percent relative estimation errors [%] (right) from the new H2-P3T3 formulations reported in Table 1.

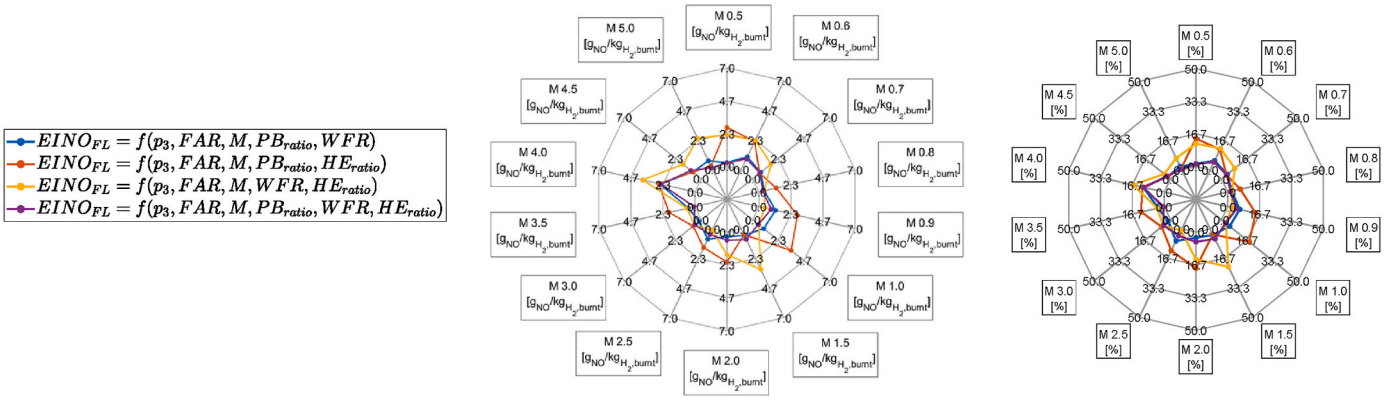

Fig. 11. Novel H2-P3T3 estimation errors evaluated for 14 Mach conditions ranging from 0.5 to 5, compared to the reference EINO from the updated emissions database: $EINO_{FL}$ absolute estimation errors [$g_{NO}/kg_{H2burnt}$] (left) and percent relative estimation errors [%] (right) from the new H2-P3T3 formulations reported in Tables 3 and 4.

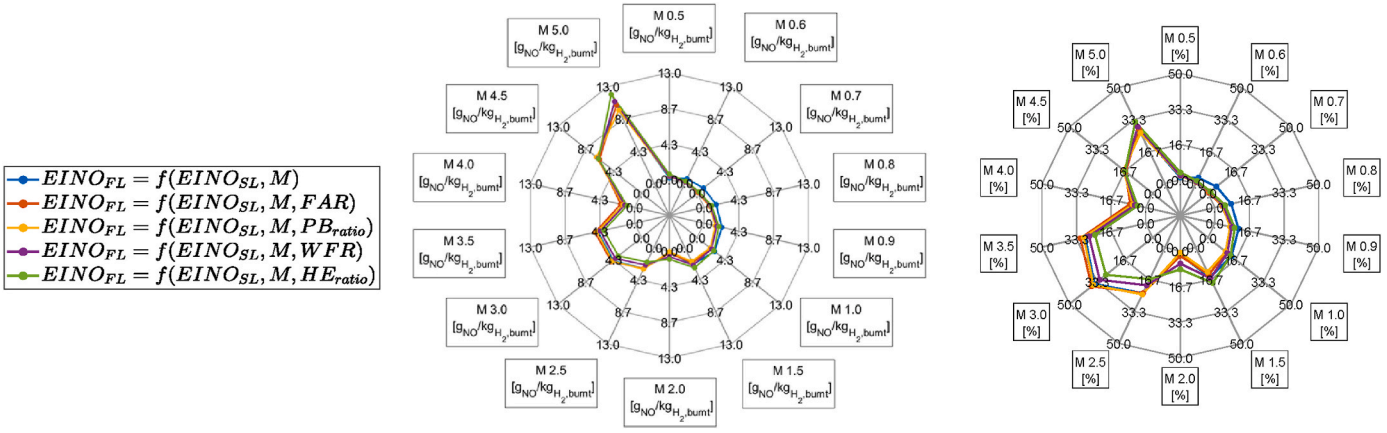

Fig. 12. Novel H2-FF estimation errors evaluated for 14 Mach conditions ranging from 0.5 to 5, compared to the reference EINO from the updated emissions database: $EINO_{FL}$ absolute estimation errors [$g_{NO}/kg_{H2burnt}$] (left) and percent relative estimation errors [%] (right) from the new H2-FF formulations reported in Table 5.

comprehensively characterize the combustion process. Moving forward with more comprehensive formulations, Fig. 13 compares the emissions estimation errors of the novel H2-FF formulations reported in Tables 6 and 7

6. Conclusions

To support and promote the aerospace sector increasing commitment towards the development of strategies for reducing emissions and mitigating environmental impact from the initial stages of the design

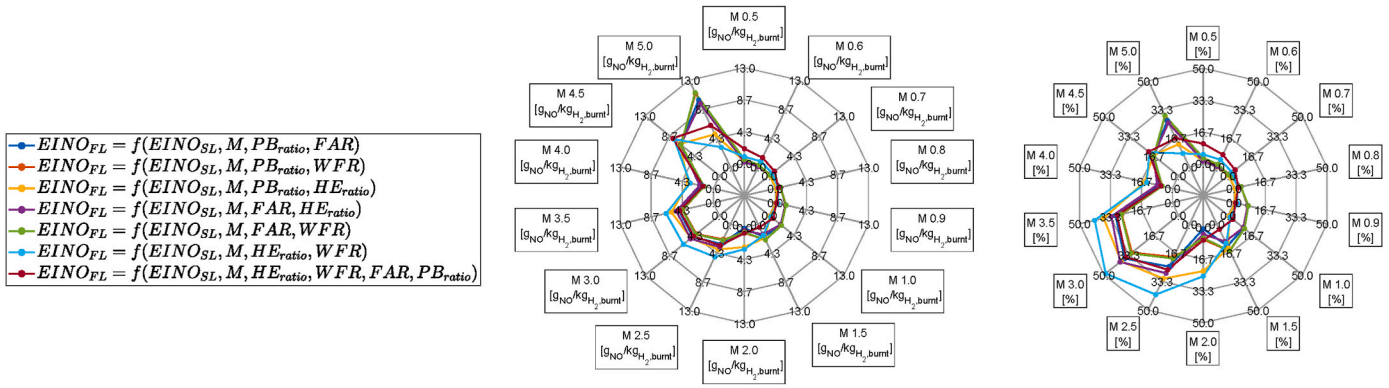

Fig. 13. Novel H2-FF estimation errors evaluated for 14 Mach conditions ranging from 0.5 to 5, compared to the reference EINO from the updated emissions database: $EINO_{FL}$ absolute estimation errors [$g_{NO}/kg_{H2burnt}$] (left) and percent relative estimation errors [%] (right) from the new H2-FF formulations reported in Tables 6 and 7.

process, this study introduces novel analytical formulations for estimating pollutants and greenhouse gas emissions from reusable access-to-space vehicles. Specifically, this research aims to expand the applicability of NO_x emissions estimation techniques originally developed for subsonic aircraft powered by conventional fuels to the Skylon Single Stage To Orbit (SSTO) vehicle. The propulsion system of this sustainable space access spaceplane, the Synergetic Air Breathing Rocket Engine (SABRE), operates in both air-breathing and rocket modes. This paper focuses on the air-breathing phase of the engine, allowing the SSTO Skylon to achieve hypersonic speed before transitioning to rocket mode. To forecast nitrogen oxide emissions during the conceptual design phase, two documented methodologies, BFFM2 and P3-T3, were selected for their accuracy and compatibility with available data in the conceptual design phase. Originally designed to assess the Emission Index of greenhouse gases and pollutants emitted by engines powered by traditional fuels for subsonic flight, these methodologies were adapted for (i) synergetic air-breathing-rocket propulsion systems for high-speed flights and (ii) hydrogen-sustainable aviation fuel. The systematic approach employed to develop these innovative formulations, H2-P3T3 and H2-FF, customized for the SABRE, is outlined. The methodology was applied to the SABRE case study, revealing the correlation between nitrogen oxides production within the engine and key chemical-thermodynamic parameters including Mach number, Fuel-to-Air ratio (FAR), airflow rate into the PreBurner (PBratio), water flow rate into the main Combustion Chamber i.e., Water to Fuel Ratio (WFR), and helium flow rate utilized for regeneratively managing the engine thermal load (HEratio). Regarding the proposed updating methodology, based on the results of the new emissions estimation formulations, the achievements and the research future developments can be summarized as follows:

- The first step of the proposed methodology for refining the P3-T3 and Fuel Flow methods for NO_x estimation from the SABRE engine involved updating the propulsion model and recalculating the engine propulsive and emissive databases. At present, this innovative engine concept has not yet entered the operational phase, resulting in the absence of official certified databases. In this regard, through the improvements made to the engine models described in the paper, the reliability level of the updated databases was enhanced. Regarding the estimation of NO_x emissions produced by the SABRE engine, although these levels are significantly higher than those documented in the literature for subsonic aircraft, they are consistent with the emission levels estimated by the designer company, REL.
- The key innovation of the proposed engine modelling strategy lies in its integrated approach, addressing both propulsion and chemical-kinetic processes. Thanks to the Cantera Matlab interface, it was possible to propose an initial version of a unified propulsive-emissive model of the engine. This model integrates the thermodynamic cycle analysis of the engine with chemical equilibrium condition simulations of the combustion process, thereby enhancing results reliability. However, given the current limitations of the Cantera Matlab interface *3.0.0*, it is necessary to utilize the Python interface for kinetic-chemical combustion simulations, enabling a higher level of accuracy in emission estimates. Transitioning to a fully Python-based model would not only convert the models to an open-access programming language but also significantly reduce simulation times. Thus, developing a unified tool with a seamless flow of information for thermodynamic and chemical-kinetic modeling of the engine, capable of automatically and simultaneously generating both the propulsive and emission inventories, promises to reduce simulation time and risk of errors (due to manual data transcription) and remains a milestone for the future evolution of this research.”.
- The H2-P3T3 and H2-FF estimation techniques follow a similar methodology to the original P3-T3 and BFFM2 methods, predicting in-flight emissions by adjusting sea-level data. The introduction of new parameters has increased accuracy but also complicated the process due to limited data availability. Indeed, the results of these new formulations indicate a significant reduction in absolute estimation errors for both H2-P3T3 and H2-FF compared to the original methods. Simultaneously, as the number of introduced parameters increases, the application of the methods becomes more challenging due to the lack of publicly available data.
- The original methods involve a single analytical formulation with adjustable parameters to effectively model various engine architectures. In contrast, the new H2-P3T3 and H2-FFM methods offer multiple formulations tailored for the same engine architecture (SABRE). This provides greater flexibility in applying the two methods, as it allows for selecting which formulation to use not only based on available data but also depending on specific requirements for more accurate modelling.
- As already documented for the original P3-T3 and FF methods, the H2-P3T3 has demonstrated greater accuracy in emission estimation resulting from the new formulations compared to those of the H2-FF. Therefore, the accuracy gap observed in the updated methods is considered reasonable. Furthermore, the reduction in estimation error compared to the original formulations for both H2-P3T3 and H2-FF confirms the effectiveness of the adaptation strategy of the estimation method to the case study, regardless of the initial emission estimation techniques.
- To refine the emission estimation strategy proposed for the SABRE and ensure its applicability to other case studies, including a new category of RLV, it is essential to investigate and resolve the physical-mathematical inconsistencies that have emerged during the analysis of the results from the new mathematical formulations. Indeed, the purely mathematical optimization of coefficients in these new

formulations has sometimes proven inconsistent with physical expectations derived from the analysis of correlations between engine chemical-propulsion parameters and emission profiles during the mission. Addressing these inconsistencies can enable the development of a unified formulation for these new methods that align mathematically with the chemical-physical expectations based on correlation analysis.

- The SABRE case study allows the emission estimation strategy to expand beyond air-breathing concepts to include the engine rocket mode. Upcoming developments in the SABRE engine announced by REL will require further updates to propulsion and emission models, highlighting the value of the versatile emission estimation strategy, which can accommodate unplanned design changes.

The proposed methodology can be considered as a general framework to adapt classical analytical formulations for emission estimation to other innovative engine configurations characterized by different requirements. This flexibility is achievable thanks to the versatility of the two software tools used for propulsion and emission modelling. Furthermore, the developed analytical formulations can quantitatively support trade-off analysis during the definition phase of propulsive architectures, alongside considerations of costs and consumption as discriminants.The authors believe that the impact of these new formulations for emission estimation on the conceptual design stage is twofold. (i) At the moment these novel formulations allow for a-posteriori assessment of nitrogen oxide emissions at a very early design stage. The newly derived formulations for the P3-T3 and FF methods represent an effective mathematical tool for the immediate and preliminary estimation of emissions. These tools can be utilized in the short term to easily and rapidly estimate emissions from already operational high-speed assets or in advanced design stages. (ii) However, the availability of these novel formulations paves the way towards a paradigm shift in conceptual design, enabling a design-to-sustainability approach. In the long term, the novel formulations can be integrated within the conceptual design framework for high-speed vehicles, enabling the verification of the compliance against future environmental sustainability requirements. The authors are currently working on this last point. Therefore, these new analytical estimation formulations can significantly contribute to proactively reducing engine emissions. Indeed, integrating these simplified formulations into emission minimization route optimization strategies can enable emission reduction right from the outset of the design process [44–50].

CRediT authorship contribution statement

Roberta Fusaro: Writing – review & editing, Supervision, Project administration, Conceptualization. **Fabrizio Borgna:** Writing – review & editing, Writing – original draft, Visualization, Validation, Software, Resources, Project administration, Methodology, Investigation, Funding acquisition, Formal analysis, Data curation, Conceptualization. **Nicole Viola:** Writing – review & editing, Supervision, Project administration, Conceptualization. **Guido Saccone:** Writing – review & editing, Supervision, Software, Conceptualization.

Declaration of competing interest

The authors declare that they have no known competing financial interests or personal relationships that could have appeared to influence the work reported in this paper.

References

[1] United Nations Framework Convention on Climate Change (FCCC), Session and Meeting Reports. UN Climate Change Conference, United Arab Emirates, 30 November to 12 December 2023.

[2] Y.Y. Lai, E. Christley, A. Kulanovic, C.C. Teng, A. Björklund, J. Nordensvärd, E. Karakaya, F. Urban, Analysing the opportunities and challenges for mitigating the climate impact of aviation: a narrative review, Renew. Sustain. Energy Rev. 156 (2022) 111972.

[3] V. Grewe, A. Gangoli Rao, T. Grönstedt, C. Xisto, F. Linke, J. Melkert, J. Middel, B. Ohlenforst, S. Blakey, S. Christie, et al., Evaluating the climate impact of aviation emission scenarios towards the Paris agreement including COVID-19 effects, Nat. Commun. 12 (2021) 3841.

[4] L. Miraux, Environmental limits to the space sector's growth, Sci. Total Environ. 806 (Pt. 4) (2022) 150862.

[5] European Space Policy Institute (ESPI), ESPI Report 90 - Bridging the Financing Gap in the European Space Sector: Alternative funding pathways in tightening markets - Full Report (2024).

[6] J.A. Dallas, S.A. Raval, J.P. Gaitan, S. Saydam, A.G. Dempster, The environmental impact of emissions from space launches: a comprehensive review, J. Clean. Prod. 255 (2020) 120209.

[7] ESA Space Debris Office. ESA'S ANNUAL SPACE ENVIRONMENT REPORT 2023 (2023).

[8] M.N. Ross, P.M. Sheaffer, Radiative forcing caused by rocket engine emissions, Earth's Future 2 (2014) 177–196.

[9] G.J. Dominguez Calabuig, L. Miraux, A.R. Wilson, A. Sarritzu, A. Pasini, Eco-design of future reusable launchers: insight into their life cycle and atmospheric impact. EUCASS2022-7353, 9TH European Conference for Aeronautics and Space Sciences, 2022. Lille, France.

[10] Y. Yan, Z. Liu, J. Liu, Computational analysis of ammonia-hydrogen blends in homogeneous charge compression ignition mode of engine operation, Process Saf. Environ. Protect. 190 (Part A) (2024) pp1283-1272.

[11] Y. Yan, T. Shang, L. Li, Z. Liu, J. Liu, Assessing hydrogen–ammonia ratios to achieve rapid kernel inception in spark-ignition engines, ASME Journal of Energy Resources Technology 146 (6) (2024) 062301.

[12] R. Yang, Z. Liu, J. Liu, The methodology of decoupling fuel and thermal nitrogen oxides in multi-dimensional computational fluid dynamics combustion simulation of ammonia-hydrogen spark ignition engines, Int. J. Hydrogen Energy 55 (2024) 300–318. ISSN 0360-3199.

[13] Z. Stępień, A comprehensive overview of hydrogen-fueled internal combustion engines: achievements and future challenges, Energies 14 (20) (2021).

[14] D. Cecere, A. Ingenito, E. Giacomazzi, L. Romagnosi, C. Bruno, Hydrogen/air supersonic combustion for future hypersonic vehicles, Int. J. Hydrogen Energy 30 (2011) 11969–11984.

[15] Y. Tsujikawa, G.B. Northambi, Effects of hydrogen active cooling on scramjet engine performance, Int. J. Hydrogen Energy 21 (1996) 299–304.

[16] G. Saccone, M. Marini, Chemical-kinetic analysis of high-pressure hydrogen ignition and combustion toward green aviation, Aerospace 11 (112) (2024).

[17] International Air Transport Association (IATA), FACT SHEET 7: Liquid hydrogen as a potential low- carbon fuel for aviation (2020).

[18] Y. Bicer, I. Dincer, Life cycle evaluation of hydrogen and other potential fuels for aircrafts, Int. J. Hydrogen Energy 42 (16) (2017) 10722–10738.

[19] K.N. Tait, M.A.H. Khan, S. Bullock, M.H. Lowenberg, D.E. Shallcross, Aircraft emissions, their plume-scale effects, and the spatio-temporal sensitivity of the atmospheric response: a review, Aerospace 9 (355) (2022).

[20] A. Mahashabde, P. Wolfe, A. Ashok, C. Dorbian, Q. He, A. Fan, S. Lukachko, A. Mozdzanowska, C. Wollersheim, S.R.H. Barrett, M. Locke, I.A. Waitz, Assessing the environmental impacts of aircraft noise and emissions, Prog. Aero. Sci. 47 (1) (2011) 15–52.

[21] J. Pletzer, D. Hauglustaine, Y. Cohen, P. Jöckel, V. Grewe, The climate impact of hydrogen-powered hypersonic transport, Atmos. Chem. Phys. 22 (Issue 21) (2022) 14323–14354.

[22] A. Ingenito, Impact of hydrogen fueled hypersonic airliners on the O3 layer depletion, Int. J. Hydrogen Energy 43 (50) (2018) 22694–22704.

[23] J. Zhang, D. Wuebbles, D. Kinnison, S.L. Baughcum, Stratospheric ozone and climate forcing sensitivity to cruise altitudes for fleets of potential supersonic transport aircraft, J. Geophys. Res. Atmos. 126 (16) (2021) e2021JD034971.

[24] N. Chandrasekaran, A. Guha, Study of prediction methods for NOx emission from turbofan engines, J. Propul. Power 28 (2012) 170–180.

[25] Intergovernmental Panel on Climate Change, Aviation and the Global Atmosphere: A Special Report of the Intergovernmental Panel on Climate Change - Engine Emissions Database and Correlation, Cambridge University Press, 1999. Issue 7.7.

[26] S. Villette, D. Adam, A. Alexiou, N. Aretakis, K. Mathioudakis, A simplified chemical reactor network approach for aeroengine combustion chamber modeling and preliminary design, Aerospace 11 (Issue 22) (2024).

[27] I.C.A.O. Icao, Annex 16 Volume II Aircraft Engine Emissions, ICAO, Montreal, Canada, 2014.

[28] N. Viola, R. Fusaro, G. Saccone, V. Borio, Analytical formulations for nitrogen oxides emissions estimation of an air turbo-rocket engine using hydrogen, Aerospace 10 (2023) 909.

[29] D. DuBois, G.C. Paynter, Fuel flow Method2 for estimating aircraft emissions, SAE Trans. 115 (2006) 1–14.

[30] A. Dinc, NOx emissions of turbofan powered unmanned aerial vehicle for complete flight cycle, Chin. J. Aeronaut. 33 (2020) 1683–1691. ISSN 1000-9361.

[31] Y. Wang, H. Yin, S. Zhang, X. Yu, Multi-objective optimization of aircraft design for emission and cost reductions, Chin. J. Aeronaut. 27 (2014) 52–58. ISSN 1000-9361.

[32] R. Fusaro, N. Viola, D. Galassini, Sustainable supersonic fuel flow method: an evolution of the boeing fuel flow method for supersonic aircraft using sustainable aviation fuels, Aerospace 8 (2021) 331.

[33] Reaction Engines Limited. SKYLON User's Manual. Doc. No. SKY-REL-MA-0001, Revision 2 (2014).

[34] S. Feast, The synergetic air-breathing rocket engine (SABRE) - development status update. IAC-20-C4-7-1, 71st International Astronautical Congress – the, CyberSpace Edition, 2020, pp. 12–14.
[35] R. Varvill, I. Duran, A. Kirk, S. Langridge, O. Nailard, R. Payne, H. Webber, SABRE TECHNOLOGY DEVELOPMENT: STATUS AND UPDATE, EUCASS2019-0307, 8TH EUropean Conference For Aeronautics and Space Sciences, Madrid, Spain, 2019, .
[36] G. Grimaldi, Development of a conceptual design tool to predict performance and pollutant and GHG emissions of high-speed vehicles using liquid hydrogen, Master's Degree Thesis. Politecnico di Torino, Torino (2021).
[37] R. Fusaro, G. Saccone, N. Viola, NO_x emissions estimation methodology for air-breathing reusable access to space vehicle in conceptual design, Acta Astronaut. 216 (2024) 304–317.
[38] A. Vincent-Randonnier, V. Sabelnikov, A. Ristori, N. Zettervall, C. Fureby, An experimental and computational study of hydrogen–air combustion in the LAPCAT II supersonic combustor 37 (3) (2019) 3703–3711.
[39] N. Zettervall, C. Fureby, A computational study of ramjet, scramjet and dual-mode ramjet combustion in combustor with a cavity flameholder. AIAA Aerospace Sciences Meeting, 2018. Kissimmee, Florida.
[40] V. Fernandez-Villace, Simulation, design and analysis of air-breathing combined-cycle engines for high speed propulsion, Doctoral Thesis. Universidad Politécnica de Madrid, Madrid, 2013.
[41] M.J. Landman, M.A.F. Derksen, J.B.W. Kok, Effect of combustion air dilution by water vapor or nitrogen on nox emission in a premixed turbulent natural gas flame: an experimental study, Combust. Sci. Technol. 178 (4) (2006) 623–634.
[42] F. Borgna, V. Borio, R. Fusaro, N. Viola, G. Saccone, Propulsive and combustion modelling of SABRE engine in air-breathing mode to support NOx emissions estimation in conceptual design, IAC-24-C4.7.12x85916, 75th International Astronautical Congress (IAC) (2024) 14–18. Milan, Italy.
[43] F. Borgna, V. Borio, R. Fusaro, N. Viola, G. Saccone, Analytical formulations for NOx emissions prediction of a SABRE engine. HiSST-2024-0344, 3rd International Conference on High-Speed Vehicle Science Technology, 2024, pp. 14–19. Busan, Korea,.
[44] M. Niklaß, B. Lührs, V. Grewec, K. Dahlmann, T. Luchkova, F. Linke, V. Gollnick, Potential to reduce the climate impact of aviation by climate restricted airspaces, Transport Pol. 83 (2017) 102–110.
[45] F. Yin, V. Grewe, F. Castino, P. Rao, S. Matthes, K. Dahlmann, S. Dietmüller, C. Frömming, H. Yamashita, P. Peter, E. Klingaman, K.P. Shine, B. Lührs, F. Linke, Predicting the climate impact of aviation for en-route emissions: the algorithmic climate change function submodel ACCF 1.0 of EMAC 2.53, Geosci. Model Dev. (GMD) 16 (11) (2023) 3313–3334.
[46] M.O. Kohler, G. Radel, K.P. Shine, H.L. Rogers, J.A. Pyle, Latitudinal variation of the effect of aviation NOx emissions on atmospheric ozone and methane and related climate metrics, Atmos. Environ. 64 (2013) 1–9.
[47] J. Faber, D. Greenwood, D. Lee, M. Mann, P.M. de Leon, D. Nelissen, B. Owen, M. Ralph, J. Tilston, A. van Velzen, G. van de Vreede, Lower NOx at higher altitudes - policies to reduce the climate impact of aviation NOx emission (2008). CE Delft: Delft, The Netherlands, Publication number: 08.7536.32.
[48] V. Kumar, P. Sharma, R. Chinnappa Naidu, M. Kaleem Khodabux, K. Sewraj, A. Anand Mohajeer, Airplane flight route optimization problem with multi-constraints. Second International Conference on Advances in Electrical, Computing, Communication and Sustainable Technologies (ICAECT), 2022, pp. 1–6. Bhilai, India.
[49] V. Ho-Huu, S. Hartjes, H.G. Visser, R. Curran, An optimization framework for route design and allocation of aircraft to multiple departure routes, Transport. Res. Transport Environ. 76 (2019) 273–288.
[50] F. Vergnes, J. Bedouet, X. Olive, J. Sun, Environmental impact optimisation of flight plans in a fixed and free route network. 10th International Conference for Research in Air Transportation, University of South Florida, Tampa, United States, 2022.